A Megathrust earthquake as source of a Pre-Colombian tsunami in Lesser Antilles: Insight from sediment deposits and tsunami modeling

L. Cordrie, N. Feuillet, A. Gailler, M. Biguenet, Eric Chaumillon, P. Sabatier

Earth-Science Reviews
May 2022, Volume 228, Pages 104018 (27p.)
https://doi.org/10.1016/j.earscirev.2022.104018
https://archimer.ifremer.fr/doc/00764/87631/

A Megathrust earthquake as source of a Pre-Colombian tsunami in Lesser Antilles: Insight from sediment deposits and tsunami modeling

Cordrie L. [1, 2, *], Feuillet N. [2], Gailler A. [1], Biguenet M. [3, 4], Chaumillon E. [3], Sabatier P. [3, 4]

[1] CEA, DAM, DIF, F-91297 Arpajon, France
[2] Université de Paris, Institut de physique du globe de Paris, CNRS, F-75005 Paris, France
[3] Université de la Rochelle, UMR 7266 LIENSs, 2, rue Olympe de Gouges, 17000 La Rochelle, France
[4] Univ. Grenoble Alpes, Univ. Savoie Mont Blanc, CNRS, EDYTEM, Bâtiment « Pôle Montagne », 5 bd de la mer Caspienne, 73376, Le Bourget du Lac cedex, France

* Corresponding author : L. Cordrie, email address : louise.cordrie@gmail.com

Abstract :

No megathrust earthquake similar to the Magnitude class 9 events in Sumatra in 2004 or in Japan in 2011 was firmly reported at the Lesser Antilles subduction zone. The largest known tsunamis followed either a strong intraplate earthquake (1867, Virgin Islands) or were transoceanic due to the 1755 Lisbon earthquake. In this region, where the convergence rate between the American and Caribbean plate is low, the recurrence time of large earthquakes may be long (several centuries or millennia) and the historical record of such events is short. It is thus difficult to estimate their impact and becomes crucial to gain information from longer-term geological records and tsunami modeling. An increasing number of old prehistoric tsunami deposits have been identified in recent years on several islands in the northern segment of the Lesser Antilles arc, between Antigua and Puerto-Rico, in Anegada, St-Thomas (Virgin Islands), Anguilla and Scrub islands. Here, we carefully review all those studies and evidenced that most tsunami deposits are about 500 to 800 years old (1200 to 1500 cal yrs. CE) likely suggesting a large event or a cluster of events at that time. We combined information provided by the sedimentological records (distribution and altitude of the sediment deposits) and tsunami models to discuss the origin of the middle age Pre-Colombian event(s). We listed all faults as possible sources of tsunamis in this complex tectonic region. We performed 35 run-up models by using high-resolution/topographic grids to compare the simulated wave heights and run-up distance to the sediment record. We showed that few models are able to generate tsunami waves which heights and run-up distances match the characteristic of the observed tsunami deposits. These models are Magnitude class 9 M-thrust earthquakes rupturing the subduction interface between 30 km in depth to the trench facing Anegada Island. Magnitude class 8 outer-rise earthquakes, modeled along the trench, are other candidates for the Pre-Columbian event(s) although less convincing than the mega-thrust ones. The realism of these models is discussed in the light of the recent coupling models of the subduction zone based on short-term geodetic records. Finally, considering all the results and data, the equally strong hypothesis that these sediments were deposited by one or several storms remains less convincing than our tsunamigenic earthquakes scenarios. We conclude that the occurrence of one or several large megathrust or outer-rise earthquakes in association with damaging tsunamis likely have occurred in the past in the Lesser Antilles and could occur again in the future. This

opens the discussion on the threat posed by such catastrophic event in these densely populated and touristic regions.

Keywords : Tsunami, Subduction, Sediments deposits, Lesser Antilles, Pre-Columbian, Fault models, Simulation

Introduction

The Lesser Antilles subduction zone is one of the most seismically quiet worldwide. The convergence rate between the North and South American and the Caribbean plates is low (~2 cm/year) and most damaging earthquakes reported in the Lesser Antilles Arc in the last decades are either shallow crustal events, in the overriding plate or deep intraslab events (Feuillet et al., 2011b), Figure 1. No megathrust earthquake similar to the Sumatra 2004 or the Japan 2011 events was firmly documented in the historical record and none was associated with a huge tsunami. However, six large M7-8 class damaging earthquakes have been reported: on April 5 1690 near Barbuda (Ms~8.0), on February 8 1843 near Guadeloupe

(Ms>8.0), on November 18 1867 near the Virgin Islands (Ms~7.2), on January 11 1839 offshore Martinique (Ms~7.8), on December 25 1969 offshore Guadeloupe (Mw=7.2) and on October 8 1974 near Antigua (Mw=7.5). Among them, the 1839 and 1843 events are strongly suspected to be interplate earthquakes (Feuillet et al., 2011b). Whereas the 1867 Virgin Island earthquake generated an important tsunami with nearshore waves of about 10 m that devastated the closest islands (Sainte-Claire Deville 1867; Reid and Taber 1920), the 1843 one likely promoted a small tsunami only, with no damage reported in English bay in Antigua (Antigua Weekly Register, 1843; Sainte-Claire Deville, 1843). In the region, the historical catalog of telluric events only goes back to 1690 but increasing evidence of an older prehistoric event are identified in the geological records (Biguenet et al., 2021; Fuentes et al., 2017; Atwater et al., 2017). Pre-Columbian sand deposits and coral boulders (dated from a period between 1200 AD and 1500 AD) were found along the coast and in several ponds in the northern part of the Lesser Antilles Arc (Anguilla) (Biguenet et al., 2021), in the Virgin Islands (Anegada and Saint-Thomas) (Atwater et al., 2017; Fuentes et al., 2017) and Puerto Rico (Donnelly and Woodruff, 2007) attesting for a main event in the area, possibly located on the northern portion of the trench. This segment of the subduction zone is strongly curved implying that the convergence is quasi frontal offshore Antigua and highly oblique offshore Puerto Rico (Figure 1). This generates an intense slip partitioning and strike-slip faults parallel to the trench in the prism and the arc. In addition, numerous oblique and normal faults (limiting deep basins) cut across the overriding Caribbean plate perpendicularly to the trench (Figure 1) and accommodate this main transition in convergence style (Feuillet et al., 2011; Laurencin et al., 2018, 2019). The very low slip deficit detected with GPS measurements along the plate interface (Symithe et al., 2015, van Rijsingen et al., 2020), suggests that the interface from Guadeloupe to Puerto-Rico is uncoupled at least at short time scale implying that this plate boundary is not able to promote a large thrust event or may hold the characteristics of a very long seismic cycle (Symithe et al., 2015). Identifying the source of this potential major Middle-Age and Pre-Colombian event is crucial to better understand the seismic cycle of this plate interface and the seismic hazard associated. Here, we 1/ review

sedimentary evidence of this pre-Columbian tsunami in the Lesser Antilles, 2/ list all the potential faults that could trigger an earthquake in the area encompassing the three islands of Anguilla, Anegada and Saint-Thomas 3/ perform tsunami simulations using high-resolution grids, and 4/ use run-up models to compare the simulated wave heights with all the deposits locations heights to conclude on the most probable source and magnitude of this event.

I - Historical earthquakes and tsunamis

The volcanic arc of the Lesser Antilles results from the subduction of the South and North American plates under the Caribbean plate at a rate of ~2 cm/y in a southwestward direction (Demets et al., 2000), In the northern part of the arc, towards the Virgin Islands, the curvature of the arc and consequently the obliquity of the convergence increases and the tectonic deformation becomes complex. Numerous intraplate faults cut across the overriding plate and represent significant sources of potential crustal shallow earthquakes (Feuillet et al., 2002, 2011b). Those events are dominant in the historical catalog with most of the main events (Mw>5) having likely ruptured intraplate faults during the last century (Feuillet et al., 2011b): in 1690 (M~8, near Barbuda), in 1935 (Mw=6.2, near Montserrat), in 1950 and 1961 (Mw=6.0 and Mw=5.5 near Nevis and Saint-Kitts), in 1969 (Mw=7.5 near Barbados), in 1974 (Mw=7.4 between Barbuda and Antigua), in 1985 (Mw=6.3 near Redonda) and in 2004 (Mw=6.3 near Les Saintes) (Figure 1). Only the largest January 11, 1839 and February 8, 1843 Magnitude 8 class earthquakes may have been large thrust events at the subduction plate interface. Their sources are however still debated (Feuillet et al., 2011b, Hough, 2011). The January 11, 1839 earthquake occurred east of Martinique and was felt in the surrounding islands with an intensity of VIII to IX (estimated magnitude of 8.0; Feuillard, 1985 and Robson, 1964). Fort De France, the main city of Martinique, was destroyed and several hundred people were killed. The 8 February 1843 earthquake occurred offshore between Guadeloupe and Antigua, the two most damaged islands, destroyed the city of Pointe-à-Pitre and killed more than 1500 people. The intensities estimated at IX in a large part of the arc between Dominica and Nevis

and at II in New York City imply a large source of magnitude between 8.0 and 8.5 (Robson, 1964 and Shepherd and Lynch 1992, Feuillet et al., 2011b, Hough 2011).

Among those events, only five earthquakes generated an observable tsunami on the closest islands (Shepherd and Lynch, 1992) (Figure 1). The 1843 earthquake was followed by a 0.5-1.2 m high tsunami wave in Guadeloupe and Antigua (Antigua Weekly Register, 1843; Sainte-Claire Deville, 1843). The Mw=7.0 earthquake of 1867, which occurred in the Virgin Island Basin generated up to 10 m-high waves in the Virgin Islands (Sainte-Claire Deville, 1867; Landers et al., 2002; Reid and Taber, 1920). The deep Mw=7.5 intraplate earthquake of 1969 was followed by a weak 10-40 cm tsunami recorded in Barbados, Antigua and Dominica (Shepherd, 2001; Stein et al., 1982). A 10 cm tsunami was recorded after the Mw=6.3 Redonda earthquake of 1985 (Landers et al., 2002). The most recent occurred in 2004. The population reported waves reaching more than 2 m in Les Saintes and 50 cm in the South of Guadeloupe (Zahibo et al., 2005; Le Friant et al., 2008; Cordrie et al. 2019). The archipelago has also been affected by a trans-atlantic tsunami generated offshore Lisbon on November 1st 1755. The tsunami waves more than 10 m-high along the Portugal coasts reached the Antilles coasts around 10 h after the earthquake. In the entire arc, observations of several meters-high waves and run-up were reported with numerous inundations of the islands' lowlands (Robson 1964, Zahibo et al., 2005). Several authors performed trans-atlantic far-field tsunami modeling to check the reliability of their source against the NW Atlantic coast tsunami data (Barkan et al., 2009; Roger et al., 2010; 2011; Clouard et al., 2017; Paris et al., 2021). The historical observations are well reproduced by the tsunami simulations generated by a source located across the ocean and they bring a deeper understanding of the marine submersion and sediment transport associated to this event (Clouard et al., 2017; Paris et al., 2021).

II – Sediment records of a Pre-Colombian tsunami

Recently, the study of five sediment cores sampled in the islands of Anguilla and Scrub during a fieldwork in March 2018 revealed the presence of a 1200-1500 cal yr CE tsunami (Biguenet et al., 2020) coeval both with a Pre-Colombian tsunami deposits found farther north in the Virgin islands (in Anegada and Saint-Thomas) (Atwater et al., 2017; Fuentes et al., 2017) and with evidences of extreme marine submersion events in Saint-Martin, Antigua, Culebra, Jamaïca, the ABC islands and further places (Bertran et al., 2004; Malaize et al., 2011; Well et al., 2017; Bain et al., 2010, 2016; Burn et al., 2017; Donnelly et al., 2005; Palmer et al., 2020; Scheffers et al., 2002, 2006; Radtke et al., 2003; Morton et al., 2006; Engel et al., 2016). Starting from Anguilla and Scrub sediment records, we reviewed all the tsunami deposits dated from this age in the surrounding islands presented in Figures 2 and 3 and listed in Table 1.

a) Anguilla and Scrub

Anguilla Island displays an asymmetric geomorphology with a very steep northern coast with 10 to 20 meters high cliffs and a low-lying southern coast along which were several ponds developed (Figure 4). Eastward, the small Scrub Island has a gentler topography with pocket beaches and several ponds and lagoons. Numerous boulders, clasts and sand layers, were detected all along the coast of Anguilla and Scrub islands and were inferred to be tsunami deposits (Scheffers et al., 2006). The analysis of the three and two cores sampled in Anguilla (Long Pond, Biguenet et al., 2020) and in the western most lagoon of Scrub (Biguenet et al., 2021) revealed the presence of 1364-1469 and 1471-1643 cal yrs CE old tsunami deposits. Anguilla Long Pond and Scrub Lagoon are separated from the sea respectively by 2-3 m and 3-4 m high barriers (Figure 4), which are therefore the minimum heights of the extreme waves that generated these deposits.

b) Anegada

Anegada is also a low-lying limestone island on which many salt-ponds have developed.

Enormous amounts of scattered clasts were identified mainly on the north part the Island (Atwater et al., 2017) with more than 200 coral boulders (brain corals and other coral species), limestone slabs, limestone boulders and cobbles. Some of them were found 1 to 2 km inland and most of the boulders (whose diameter range between 0.3 m and 2.7 m) were found several meters above sea level behind 2-6 m high ridges (Figure 5). Radiocarbon ages obtained from 36 clasts (corals, valves, shells) associated to a main sand sheet yield the range of 1000-1500 cal yrs CE, and the radiocarbon ages obtained from 16 brain corals correspond to a period of 1200-1480 cal yrs CE, a period also indicated by the age of the brain coral clasts, conch shells, and by the youngest of the lucina ages. This 1200-1480 time window likely applies to initial emplacement of the inland fields of scattered limestone boulders and cobbles.

Another sand and shell sheet is bracketed by radiocarbon dating and historical evidence in the range 1650–1800 cal yr CE. The flooding in 1650–1800 is associated with the tsunami of Lisbon in 1755, the waves may have risen gradually against beach ridges of the north shore without transporting coarse clasts from the reef and merely reworked the, already in place, smaller limestone clasts. This overwash event was much less powerful than the 1200-1480 Pre-Colombian one which likely resulted into the entrainment of coral clasts and mollusks from the fringing reef including 0.3 m to 2.7 m diameter coral boulders, into the abundant breaching of beach ridges and into a flow that probably crossed the island from north to south reaching heights of at least 4 m and deposited of a sandy fan with clasts and shells near the south shore. The origin of this event is unsure, it was either a tsunami of nearby origin or an unusual storm but its impact at Anegada largely exceeded any overwash event that may have occurred in the last 500 years, even the 1755 one.

c) Saint-Thomas

Sediment cores sampled in four coastal ponds and one mangrove on Saint-Thomas Island (Fuentes et al., 2017) showed five unusual overwash deposits (Figure 6). Their mixed sand

composition (marine and lacustrine), the erosional contacts, the fining upward sequences and sometimes the presence of a mud cap are interpreted by the authors as evidence of tsunami deposits. In comparison with other overwash layers showing sharp but not erosive contacts or only lacustrine composition and that are interpreted as storm deposits. The tsunami deposits are composed of mixed lithic and carbonate sand, marine shell, coral boulders and fragments. One of them is dated between 1200 and 1450 cal yrs CE and has been identified at all the five studied sites covering a 25 km long and 10 km large area, suggesting that it had a significant impact (Fuentes et al., 2017). Moreover, the five ponds are separated from the sea by 2 m high barriers (Figure 6), the minimum height of the waves that impacted the island at that time.

d) Tsunami or storm deposits and discontinuities

Other Pre-Colombian traces of extreme overwashes have been identified in the surrounding islands of Culebra, Saint-Martin, Antigua and Barbuda. Their origin (storm or tsunami) is uncertain but in the light of new finding from sediment cores in the Virgin Islands, it cannot be excluded that they may correspond to the same Pre-Colombian tsunami.

Three cores of sediment were sampled in Big Culebrita Salt Pond, a pond located on the northwestern tip of Culebra Island (Donnelly et al., 2005, Figure 2). Several layers were interpreted as storm deposits, but the authors do not exclude the possibility of tsunami deposits. One layer, above another 692-793 cal yrs BP old one is particularly thick (15-20 cm) and presents abrupt contacts with the underlying and overlying layers. It is made of sandy shell and was observed on the three cores. The clay around this layer was reworked during its deposition. Using Calib 8.2 Marine20 calibration curve, we obtained a maximum age of 1100-1300 cal yrs CE for this deposit.

Many transported boulders were identified along the coastline of Saint-Martin, the largest one being located on the westernmost peninsula at 6 m above sea level (Scheffers et al., 2006). However, most of the tsunami traces (boulders and sand deposits) are located on the

opposite eastern shore, on a small island at the entrance of Baie de l'Embouchure. Three cores were sampled in a pond located in the northern part of the island (Bertran et al., 2004 - Malaize et al., 2011) and chronology on those sediments yielded ages between 1000 and 1800 cal yr CE. The sedimentological evidence supports a storm origin for most of the deposits but the authors do not exclude that some sand layers correspond to tsunamis.

In Antigua, a core was sampled in the Nonsuch Bay, on the north-eastern coast (Well et al., 2017). One coarse sand layer with microshells and high sodium content contrasts with the rest of the core, mainly composed of clay and volcanic ashes. The authors suggest that a storm surge was responsible for this unique coarse sediment layer. This layer lies in between two layers dated at 295 and 600 Cal yr BP and correspond approximately to the range of 1350–1655 cal yrs CE, a period which fit that of the Pre-Colombian tsunami.

Samples and sediment cores were collected in Barbuda in 2010 (Bain et al., 2010; Bain et al., 2016; Burn et al., 2017). From the core analysis, the authors do not mention the possible occurrence of a tsunami (Burn et al., 2016). However, based on historical, archeological and archaeobotanical studies and the analysis of charcoal concentration in the sediments, the authors proposed that the island was abandoned around a date between 1300 and 1500 cal yrs CE (Bain et al., 2017). This could be linked to the impact or devastation of the island by an extreme event like a tsunami.

e) Regional picture

Overwash deposits have also been identified in Curaçao, Bonaire and Aruba (Figure 2), 3 islands southwest of the Lesser Antilles arc (Scheffers et al., 2002; Radtke et al., 2003; Morton et al., 2006; Engel et al., 2016). Those debris, made of boulder fields, rampart formation and ridges, are present on the northeastern coast of the three islands and reach 8 to 12 m above sea level and 400 m inland. Ages of 43 samples yielded three main time units, one of them corresponding to an age around 1250 and 1650 cal yr CE that matches the 1200-1500 cal yr CE period. The nature of the event is debated, several authors favor the

tsunami hypothesis (Scheffers, 2004; Engel et al., 2012), but other argue that storm waves would be sufficient to explain the deposits (Morton et al., 2008; Spiske et al., 2008). On the north side of the Caribbean Sea, 15 sediment cores were sampled in a pond of the southeastern coast of Jamaica (Palmer et al., 2020). One washover unit dated from 1290-1400 cal CE was identified in 13 cores, the origin is unclear, but the hypothesis of a tsunami is not excluded by the authors. The strongest tsunamigenic earthquakes of those last decades have shown that a tsunami can propagate and conserve high amplitudes far away from its source. Aruba, Bonaire, Curaçao and Jamaica are located 300 to 500 km away from the northern part of the Lesser Antilles arc, it is reasonable to assume that a major tsunami generated on the arc could propagate that far away. However, it is not evident that it could conserve sufficient energy to displace the observed amount of sediment.

The graphic presented in Figure 3 gathers all the tsunami traces of the Lesser Antilles described above. The possible paleo tsunamis identified in this region for the past millennia are few. The traces found in Saint-Thomas, Anegada and Anguilla are very close in time and in space. They could be related to one same major tsunami, but the sediment chronology provides a total period (blue shade in Figure 3) ranging between 200 to 300 years so the hypothesis of several tsunamis occurring during this period should also be considered. In both hypotheses, tsunami simulations can be used to identify the possible sources from the fault systems of the arc capable of producing the observed impact in near and far field.

III – Possible sources of tsunami

The deposits in Anguilla, Anegada and Saint-Thomas are suspected to be associated to a major tsunami which can have multiple origins. Indeed, the northern part of the arc is affected by several major active tectonic features which are possible sources for such a tsunami. There is the subduction zone with the Puerto-Rico trench associated faults, the Anegada passage composed of several grabens and normal faults perpendicular to the arc and several additional intra-arc fault systems in between the islands (Figure 1).

a) The intra-arc fault systems

The Lesser Antilles inner-arc displays two fault sets: (1) one group of trench-perpendicular normal faults along the eastern edge of the arc accommodates the trench parallel extension and (2) a set of en-echelon normal faults between Les Saintes and Redonda that accommodates left-lateral transtension (Feuillet et al., 2000, 2002, 2011). The relative plate convergence along the Antilles subduction zone is known to be smaller than that of other subduction systems with a slip-rate of 19 mm/yr (Demets et al., 2000). There is no accurate measurement of the slip-rate along the inner-arc fault system, but it is estimated to be around a few mm/yr (Leclerc et al., 2016). Given these active faults are 20-50 km long, they are potential sources of M>6 earthquakes and the slip-rate is sufficient to consider the occurrence of such intra-arc earthquakes as seriously as the occurrence of a megathrust earthquake along the subduction plate boundary.

The historical seismicity is indeed greater in the intra-arc fault systems than along the subduction contact, with several tsunamigenic earthquakes recorded in history. The 1867 earthquake of M7.0 in the Virgin Islands generated a large tsunami in the closest islands, with 10 m waves reported (Reid and Taber, 1920), occurring along some shallow normal fault systems. Similarly, the Roseau normal fault system south of Guadeloupe ruptured in 2004 and generated a tsunami in Les Saintes Island, smaller than the 1867 one but still consequent for a M6.3 earthquake. Those events show the tsunami potential of the Lesser Antilles intra-arc fault systems, it motivated us to start the study with the hypothesis of a tsunami generated by a local shallow normal fault before the mega-thrust earthquake hypothesis.

The sea-floor images of the Lesser Antilles northern segment reveal numerous traces of faults reaching the surface, structuring the carbonate platforms and cutting through the islands (Laurencin et al., 2017; Styron et al., 2020). Half of those faults are perpendicular to the arc, segment the eastern side of the carbonate platform and have seaward facing sharp

reliefs. Among them, the set of faults associated with the Anegada passage is an important source of potential ruptures including the 1867 earthquake one. This passage is cutting through the arc from the Whiting Basin at the limit of Puerto Rico micro-plate to the Sombrero Basin where the subduction front reaches its maximum curvature (Laurencin et al., 2017). It has a great influence on the dynamic of the arc evolution and is an active feature of the area. The other half of the intra-arc faults have a northwest-southeast orientation, generally parallel to the arc, located in between the islands or crossing them (Feuillet et al., 2011). Those faults are 30 to 50 km-long with a dip oriented either to the northeast or the southwest.

b) The subduction zone

The subduction beneath the Lesser Antilles arc displays heterogeneous characteristics from the northern to the southern end. The seismogenic zone is 60-65 km deep (Pauletto et al., 2017; Laurencin et al., 2018; Bie et al., 2019) with a shallow interplate seismicity observed at approximately 10 km depth (Laurencin et al., 2018). The uppermost portion of the slab (between 0 and 30 km) dips at around 10° in the North and 15° in the Central part of the arc, whereas it dips at 20° between 30 and 50 km and at 40-50° at depth larger than 50 km (Pauletto et al., 2017; Laurencin et al., 2018; Bie et al., 2019). The distribution of seismicity is heterogeneous along the arc. There are seismic gaps, particularly along the segment between Anguilla and Barbuda (McCann and Sykes 1984). The geodetic studies suggest a very low coupling along the subduction interface (Manaker et al., 2008; Symithe et al., 2015, Calais et al., 2016), meaning that no strain accumulates during the interseismic period at plate interface to be released during a future earthquake. However, this coupling rate is estimated over a short period with geodetic instruments, and this may be different over longer period of time (several decades and centuries) as inferred from coral microatoll studies (Weil-Accardo et al., 2016, Philibosian et al., 2022). Moreover, two earthquakes in 1839 and 1843, of an estimated magnitude larger than 8, are already suspected to have occurred on the interface.

c) Intraslab earthquakes

Intermediate-depth intraslab earthquakes have been identified in several subduction zones (Hasegawa and Nakajima, 2017) like Tohoku and Cascadia and associated to dehydration processes. Cascadia is particularly interesting because of its similarities with the Antilles arc: slow subduction zone with a small dip angle. Moreover, dehydration processes have been identified in the southern part of the arc (Pauletto et al., 2017) so the hypothesis of similar processes in the northern segment that would lead to a fault rupture in the slab would not be so surprising. The subduction of fractured features and reliefs alongside a slab was correlated to intermediate depth seismicity variation in Peru and Vanuatu (Kumar et al., 2016; Baillard et al., 2018). Reliefs like oceanic ridges (DER in Vanuatu) present dense fracture systems which favor the hydration of the crust prior to subduction.

Along the Antilles subduction, the prolongation of Barracuda ridge corresponds to another ridge named the Main Ridge in the northern tip of the arc. If the subducted ridge actually continues between those features, then it should be located at around 25-30 km-depth and 150 km distance from the trench. The hydration of the Barracuda Ridge has not been studied but the subduction of this relief represents another potential source of earthquake.

d) Puerto-Rico Trench and Main ridge

In the northern segment of the Lesser Antilles arc, north of Puerto-Rico, the underthrusting of the Main Ridge at the tip of the most curved part of the subduction form a complex tectonic zone with changes in fault system trends (DeMets et al., 2000; Grindlay et al., 1997; Grindlay et al., 2005). The convergence between the two plates is partly accomodated by strike-slip motion of Bunce fault along the trench and the Bowin fault, which borders the Main Ridge (Figure 1, DeMets et al., 2000; Grindlay et al., 2005). The Bowin fault is composed of one thrust fault and one back-thrust fault on both side of the ridge. This segmented fault system displays a strong reverse component with a steep dip of 60° (Grindlay et al., 2005; Ten Brink et al., 2005) and represents a potential tsunamigenic source.

In addition, seismic profiles evidence important outer-rise normal faults that bound large blocks rotated by the collapse of the trench floor (Ten Brink et al., 2005; Marcaillou et al., 2021). Bathymetric data of the northern segment of the Antilles arc (Andrew et al., 2013) reveal multiple fault scarps of 50 to 100 km length slightly oblique along the trench north-east of the Main Ridge. They also represent serious candidates of tsunamigenic source already considered in the study of Anegada's tsunami deposits (Buckley et al., 2012; Atwater et al., 2017).

e) One or several earthquakes?

As presented in the previous part, several islands of the arc present tsunami deposits dated from the same period. However, we are not able to ensure that all those traces have the same origin. Thus, we decided to model sources with a potential regional tsunami impact such as mega-thrust subduction fault but also fault candidates that generate more localized tsunami impact and that might not reach all of the three islands. So, as described in previous paragraphs, almost all the potential seismic sources in the region surrounding Anguilla, Anegada, Saint-Thomas are considered in this study. They are divided in two categories: the normal shallow faults (intra-arc fault systems, outer-rise faults, wedge faults…) and the subduction thrust faults (Table 1, Figure 7, Figure 8).

IV –Modeling Method

The initiation is the seafloor deformation generated by the rupture of fault and modeled using the Okada (Okada et al., 1985) formalism. It assumes an elastic, isotropic and homogeneous medium in which a rectangular fault ruptures with a uniform slip. It gives the ground surface displacement as a function of geometric parameters (dip, strike and slip angles, fault length and width, depth and slip dislocation) and of the surrounding rocks parameters. Compared with the tsunami velocity (0.2 km/s), the rupture velocity (about 3 km/s) is large, so the surface displacements over the faulted regions are assumed to be instantaneous with respect

to waves modeling. The sea water is considered as a homogeneous, incompressible and non-viscous fluid.

a) Characteristics of the model

Taitoko is a parallelized numerical code developed by Heinrich et al., (1998) and Hebert et al., (2001) which computes the propagation of tsunami waves generated by a seismic source (Heinrich et al., 2020). It has been applied to numerous worldwide tsunamis and has proven its efficiency, especially in the Pacific. An area where ample data are available to validate the simulation of waves triggered by historical and great earthquakes of the last decades (Hébert et al., 2007; Hébert et al., 2009; Schindelé et al., 2015; Poupardin et al., 2018). It was recently used in the study of the 2018 Palu earthquake and tsunami (Jamelot et al., 2019). The simulation is composed of three steps: the initiation of the wave, the propagation and the run-up at the coast.

This code solves nonlinear shallow water equations, written in spherical coordinates. Frequency dispersion is assumed to play a minor role since propagation distances are short. The nonlinear long wave equations are solved by means of a staggered-grid finite difference method. Nonlinear terms in the model are approximated with upwind finite differences, and linear terms are approximated by centered finite differences. The temporal scheme uses an iterative procedure and is based on a second order Strong Stability Preserving Runge Kutta method. To deal with shoaling and resonance effects of the tsunami waves, detailed bathymetric grids are used for the precise modeling of the coastline response in bays and harbors. To this end we calculate wave propagation on successive levels of nested grids of increasing resolution close to the shore, built using available bathymetric and topographic data. Open free boundary conditions are prescribed to the boundaries of the mother grid covering the studied area, and wave heights along the boundaries of a fine grid are spatially interpolated at each time step from the value computed in the coarse grid containing the fine grid.

The method takes into account the inundation of the coastal areas and allows us to compute run-up values along the first tens of meters of the nearshore topography. Numerically, this is handled by an extrapolation of the results from dry to wet nodes at the dynamic shoreline modulated by a Manning friction coefficient fixed to a reference value of 0.05.

b) Bathymetric grids

23 imbricated bathymetric grids were defined in order to cover the whole studied domain. The mother grid is a 450 m resolution grid from the 2020 Gebco database (GEBCO Compilation Group (2020) GEBCO 2020 Grid (doi:10.5285/a29c5465-b138-234d-e053-6c86abc040b9)). An intermediate grid of 100 m resolution from the SHOM database covers the area of Anguilla, Saint-Martin and Saint-Barthélemy (Shom, 2018. MNT bathymétrique de façade de Saint-Martin et Saint-Barthélemy (ProjetHomonim). http://dx.doi.org/10.17183/MNT_ANTN100m_HOMONIM_WGS84). Another 100 m-resolution grid from the SHOM database covers Guadeloupe Island (Shom, 2018. MNT bathymétrique de façade de la Guadeloupe et de la Martinique (Projet Homonim : http://dx.doi.org/10.17183/MNT_ANTS100m_HOMONIM_WGS84, Deplus 1998 : http://dx.doi.org/10.17600/98010020, Deplus et al., 2002 : http://dx.doi.org/10.17600/2010020, Feuillet 2009 : http://dx.doi.org/10.17600/9020020, Laigle et al., 2007 : http://dx.doi.org/10.17600/7010020 and Lebrun 2009: http://dx.doi.org/10.17600/9020010). A 50 m-resolution grid from the NOAA database covers the Virgin Islands (NOAA National Geophysical Data Center. 2010: St. Croix, U.S. Virgin Islands Coastal Digital Elevation Model. 2014: St. Thomas and St. John, U.S. Virgin Islands 1/3 arc-second MHW Coastal Digital Elevation Model. NOAA National Centers for Environmental Information). This study is focused on the three areas of the Lesser Antilles where most of the ~1500 cal yr CE deposits have been identified: Anguilla, Scrub, Saint Thomas and Anegada islands (Figures 4, 5, 6). A set of 1 m and 5 m resolution grids were built based on LIDAR data and DEM on each of those 3 places (Office for Coastal Management, 2021: 2011 NOAA Bathymetric Lidar: U.S. Virgin Islands - St. Thomas, St.

John, St. Croix (Salt River Bay, Buck Island), https://www.fisheries.noaa.gov/inport/item/48218.; Fredericks, X., ten Brink, U.S., Atwater, B.F., Kranenburg, C.J., and Nagle, D.B., 2016, Coastal Topography—Anegada, British Virgin Islands, 2014: U.S. Geological Survey data release, https://doi.org/10.5066/F7GM85F3.). The high resolution of those later grids enables the simulation of the run-up where tsunami deposits have been identified.

c) Coastal wave height and run-up

The high-resolution grids correspond to the present-day topography of the islands. In many locations, the continent is separated from the sea by sediment barriers that could have been built up or eroded by tsunamis or hurricanes that struck the area those past 500 years. Most of the dated deposits considered in this study are located in lagoons. Those lagoons are separated from the sea by sediment barriers (Figures 4, 5 and 6) that are generally 1 to 10 meters high. Obviously, the topographic barriers have changed during the last 500 years. Given these uncertainties on preexisting topography, we extracted the wave height modeled offshore at the base of the sediment barriers before any run-up calculations. We compare those offshore wave height values to the minimal wave height needed for the tsunami to overwash the barrier close to each sediment record used in this study.

d) Calculation of a correlation coefficient

The interpretation of all the fault models results are presented in Figure 10. The correlation coefficient represents the “goodness of fit” of the simulated wave heights compared to the topographic heights (sand barriers, cliff...) associated to each tsunami deposit. The correlation coefficients presented in Figure 9 are calculated for the results of maximum water height (offshore) reached after 2 hours of simulation. The coefficient corresponds to the comparison of the modeled water heights (hw) to the observed coastal heights (hc) for all the studied

sites. The final correlation coefficient is the mean value of this ratio (hw/hc) with the value for each site (s) and the total number of sites (N) :

$$Cw = \sum_{S} \left(\frac{h_{w_s}}{h_{c_s}} \right) / N$$

In the upper graphic in orange (histograms a of Figure 10), the coefficient is calculated using all the sites of this study. In the lower graphic in blue shades (histograms b of Figure 10), the coefficient is calculated using only the sites on one of the three islands. The Anguilla's sites in medium blue (Cw_{ang}), the Anegada's sites in dark blue (Cw_{ane}) and the Saint-Thomas sites in light blue (Cw_{tho}).

$$Cw_{ane} = \sum_{S_{ane}} \left(\frac{h_{w_s}}{h_{c_s}} \right) / N_{ane}$$

The analysis of the results independently on each island enables us to interpret the results with the hypothesis of the occurrence of not one but several tsunamis during this period of time.

V- Fault models

The fault model parameters were chosen firstly considering the tectonic and known geological structures of Antilles historical earthquakes mechanisms. In addition, in order to have more realistic ranges of parameters for modeled ruptures, we looked at historical earthquake mechanisms from other subduction zones in the world.

a) Intra-arc normal fault models

In order to generate a consequent tsunami wave, we decided to model sources of a magnitude between 7 and 8 depending on their length. Intra-arc earthquakes of this

magnitude are not frequent but are documented on other subduction zones. In New Zealand, the 2016 Kaikoura earthquake (Ulrich et al., 2018) reached a magnitude of 7.8 with a major ruptured segment of 60-80 km long and 20-30 km large and a slip range of 0 to 10 m. In Chili, an important number of crustal earthquakes occurred along the subduction zone (Santibanez et al., 2019) like the Pichilemu earthquakes of Mw6.9 and Mw7.0 in 2010 (Farias et al., 2011) or the Pisagua earthquake of 2014. Those events are all located at depth between 5 and 20 km, with a fault width of approximately 10 to 20 km and a slip of 2 m (Santibanez et al., 2019). In North America, the Cascadia earthquake that occurred in 1946 (Rogers et al., 1978) was a crustal earthquake of Mw7.2 generated by a fault of 50-70 km long, a 25-35 km-wide, at a depth of 10-40 km and an estimated slip of 2 m. Finally, some crustal earthquakes also occurred along the subduction zone of Indonesia (Hurukawa et al., 2014; Rusydy et al., 2015) with length of 60 to 150 km and depth of 15 km.

Intra-arc normal fault lengths around Anguilla vary between 80 to 100 km and display steep dip angles (45°-50°) with alternating northwest-dipping and southeast-dipping mechanisms.

Based on the tectonic features of the area presented in section III (Figure 1) and the empirical laws of Wells and Coppersmith (1994) that links the moment of the earthquake to the rupture area, the slip and the rigidity of the medium, we built 16 intra-arc fault models (Figure 8). The width, depth, dip angle, strike angle and slip intensity were fixed for all the models respectively to 20 km, 8.2 km, 45°, -90° and 2 m (Table 2), a rupture that spreads from 15 km deep to the surface, in the most brittle part of the crust. The only varying parameters of those models are the length, the position and the rake angle, all chosen based on bathymetric and seismic data. Those 16 models correspond to the maximized but realistic rupture scenario associated with each fault.

b) Subduction thrust fault models

The curvature of the arc reaches its maximum angle in the north, in front of the Virgin Islands and Puerto-Rico, a segment of the subduction where the slab is also particularly shallow

(Laurencin et al., 2019). The convergence obliquity is of 30° in the south of the arc and increases northward to more than 70° generating a left lateral motion that is accommodated by a 535 km-long strike-slip fault: the Bunce Fault (Ten Brink et al., 2004; Laurencin et al., 2017). This fault likely delimits the internal and external parts of the accretionary prism, it penetrates the prism until the top of the dipping plate (Laurencin et al., 2017). The rooting of this fault on the subduction contact under the prism could be a limit to the rupture propagation in a scenario of the accretionary prism earthquake. The trace of the Bunce fault is located between 20 and 30 km westward of the trench (Laurencin et al., 2018) and it likely joins the slab at a depth of 3.5 km considering a dip of 10°. Then a rupture from the trench surface to the Bunce fault root should have a width of 20 km. The subducting slab presents important topographic features that are the Tiburon, Barracuda and Saint-Lucia ridges. They generate a deformation of the accretionary wedge and likely affect the segmentation of the subduction contact. The segmentation of the subduction zone properties can have an impact on the rupture propagation along the contact or should be included in the choice of mega-thrust fault models. We limited the study to the northern half part of the subduction. The Barracuda ridge subduction is located eastward of Antigua and Guadeloupe at the end of the north curvature of the arc and can be considered at a first limit of segment. The Anegada passage joining the trench at the maximum of the arc curvature is another key feature that likely affects the segmentation.

Using those tectonic features, we created 6 mega-thrust fault models: 2 models (MT1 and MT2) dividing the north arc on 350 km-long segments and 4 models (T1,T2,T3,T4) subdividing it on 200 km-long segments (Figure 7). Each of those 6 segments are modeled with a width of 100 km, extending from 30 km in depth to the surface, and with a slip of 20 m. The magnitudes of our models range between 8.7 and 9.0 and the parameters are chosen following the law of Wells and Coppersmith (1994) (Table 2). Those models are comparable in size with recent mega thrust earthquakes (2004 Mw 9.0 event in Sumatra, the 2010 Mw 8.8 event in Maule (Chili) and the 2011 Mw 9.1 event in Tohoku (Japan)).

A deeper part of the contact (30-60 km depending on subduction zone) where the slab's dip increases is also the source of mega-thrust earthquakes in other subduction zones. In Chile, the events of Antofagasta in 1995 (Mw8.0) and Iquique in 2014 (Mw7.7) are examples of those "Interplate domain C" earthquakes (Ruiz S. and Madariaga R., 2018). In the Lesser Antilles, this "C domain" where the slabs dip increases from 10° to 20° (at 30 to 50 km depth) would be located just under Anegada and Anguilla islands.

So, two additional deep interplate faults (Mw8.0) are modeled based on the slab geometry and the Chilean earthquakes parameters with a length of 150 km, a slip intensity of 6 m, a depth of 40 km and a dip of 20° (IT1 and IT2, Figure 7, Table 2).

c) Wedge fault models

Another possibility of tsunamigenic earthquake is the rupture of the subduction contact beneath the accretionary prism (Wang et al., 2006). The magnitude of this type of events is smaller than a mega thrust earthquake but the combination of the very shallow location and the fault mechanism can generate a consequent tsunami. The Mentawai earthquake of 2010 with a Mw7.8, occurred beneath the accretionary prism and generated 5-10 m waves along the closest coasts (Hananto et al., 2020). The Mentawai earthquake seismologically determined coseismic slip was higher than 10 m for a dip of 6° (Hananto et al., 2020). Some joint inversions (Yue et al., 2014) yielded models of a 100 km-long and 5 km-wide surface patch with 23 m of maximum slip in addition to other deeper patches of rupture.

Based on the example of the Mentawai earthquake parameters and the Antilles prism characteristics, we selected a maximizing scenario of a 100*20 km wedge fault rupture with a slip of 20 m corresponding to a magnitude Mw8.0 earthquake. This model of rupture was simulated on 3 locations along the trench facing Anguilla and the Virgin Islands (W1,W2,W3; Figure 8, Table 2).

d) Intraslab faults

Based on the known intraslab earthquake rupture models (Hasegawa and Nakajima, 2017),

the geometry of the slab, the position of the subducted ridge and existing faults along the Barracuda Ridge and Main Ridge, we modeled two rupture scenarii (IS1 and IS2). They are localized at 40 km-depth under Anegada and Anguilla Islands and have a magnitude of Mw7.5 for a 50*20 km plane with 5 m slip (Figure 8, Table 2).

e) Puerto-Rico trench Outer-Rise and Ridge faults

Two segments lying around the Main Ridge identified in the bathymetric data and seismic profiles can be modeled (Grindlay et al., 2005; Ten Brink et al., 2005): a south-west dipping 40 km-long for 20 km-wide segment north of the ridge (Ridge1) and a north-dipping 50 km-long for 20 km-wide segment, south of the ridge (Ridge2) (Figure 8). With an average slip of 5 m, a maximizing value for crustal earthquakes, the two fault models have a magnitude of 7.3 and 7.4 respectively (R1 and R2 in Table 2). Similar faults have been identified in the Hikurangi subduction zone with 60° dipping faults that generated sequences of earthquakes (Robinson 1994).

Associated to the subduction trench, Magnitude Class 8 Outer-Rise earthquakes may occur in the Lesser Antilles. Those events are mainly characterized by normal faulting mechanisms (Craig et al., 2014). The Mw8.1 Kuril earthquake of January 2007 (200 km-long normal fault, most of the rupture in the first 30 km with an average slip of 9.6 m and a dip of 60°; Ammon et al., 2008), generated a small tsunami on Crescent coast of California. The Mw8.1 Samoa-Tonga earthquake of September 2009 (Rupture of 150*50 km, slip of 5 m, averaged depth of 5 km, dip of 30-50°; Lay et al., 2010) generated a tsunami of 10 to 20 m (due to 3 coeval seismic ruptures). The Mw7.2, Sanriku earthquake of December 2012 (50-100 km-long normal fault, average depth of 10 km with a slip between 0 and 5 m; Harada et al., 2013), but also the less known Mw8.4 Sanriku (Japan) earthquake in 1933 and Mw8.3 Sumbawa (Indonesia) earthquake in 1977, generated tsunami waves reaching heights of respectively 1 m, 28 m and 6m.

The bathymetry (Buckley et al., 2012; Atwater et al., 2017) and seismic imaging (Marcaillou et

al., 2021) of this trench area show multiple long fault traces that could be associated to past outer-rise ruptures. The seismic profiles show normal faults dipping in both directions (parallel and perpendicular to the slab) with a majority of faults dipping toward the trench. Using the same position and dimensions as the one proposed by Buckely et al. (2012) we create a Mw8.0 fault model located in front of Anegada island (OR1) with a length of 120km, a width of 45km and a slip of 7 m. This OR1 model dips toward the trench so we model the same fault with a dip opposed to the trench (OR2). The propagation of the rupture deep into the mantle has been observed for the Mw8.2 Kuril earthquake so it is acceptable to model a width of 45 to 50 km. However, the 2007 Kuril, the 2009 Tonga and the 2012 Sanriku outer-rise fault slip distributions show a concentration of 5 to 10 m slip on the most updip 10 km of the plane. So, we create a fault model closer to these slip distributions with a length of 150 km, a width of 25 km and a slip of 10 m at three different positions (OR3, OR4, OR5). The five fault models have a dip of 60° and a magnitude of Mw8.0 (OR1,OR2,OR3,OR4,OR5; Figure 8, Table 2).

V – Results

Thirty-five tsunami simulations were performed for this study. We choose here to focus on the 11 faults (W2, T1, T2, T3, T4, T2, OR1, OR2, OR3, OR4, OR5) that generate the strongest tsunami simulation in each fault category. The maximal wave heights recorded offshore (close to deposit location) for the three islands are presented in Figure 9. The interpretation of the 35 fault models results are presented in Figure 10. Calculations of the correlation coefficients are explained in the Method (Part IV). They represent the “goodness of fit” of the simulated wave heights compared to the height and position of the tsunami deposits and they are used to have a quantified evaluation of the consistency of each model. Figures 12 and 13 present in details the maximum water height maps of Anguilla, Scrub, Anegada and Saint-Thomas obtained respectively for models T2 and OR3. Figure 13 show the results of run-up on the islands of Anegada and Scrub with four profiles of maximum water heights and flow

velocities obtained for models T1, T2, OR1, OR2, OR3 and OR4.

a) Analysis of simulation results on Anguilla and Scrub Islands

The tsunami simulations on the area of Anguilla and Scrub were performed on 5 m-resolution grids and the two lagoons where sediment cores were sampled are mapped with 1 m-resolution grids. We extracted the values at the coordinates of the two ponds where tsunami deposits have been identified (Biguenet et al., 2020, 2021). In Figure 9, Scrub1 gage is located in Scrub bay, next to the lowest sand barrier's topographic height (northern part) and Scrub2 gage is located in the bay in front of the central part of the barrier. Ang1 gage is located next to the entrance of Long Pond.

The five outer-rise models (OR1, OR2, OR3, OR4 and OR5) generate tsunami wave heights at the limit or just above the barriers heights as it can be seen on Figure 9b (where the blue curves are below the black topographic threshold). The water height map of Anguilla and Scrub obtained with the fault model OR3 (Figure 12) show that the wave passes the sand barrier of Scrub and barely floods the lagoon but does not flood Anguilla's one. The resulting correlation coefficients (Figure 10) are not the highest one but are still good. The mega-thrust fault models T2 and T3, which correspond to the trench segments in front of Anguilla and Scrub islands, generate wave heights of 5 to 10 m (Figure 9a where the brown and orange curves are above the black topographic threshold) along the coast and largely exceed the topographic threshold. The correlation coefficients are very high compared to the rest of the models (Figure 10). The mega-thrust T1 and T4 models, the most distant ones, generate a smaller tsunami. The water height map of Scrub obtained with the fault model T2 (Figure 11) shows that the waves largely pass the sand barrier of Anguilla Long Pond and Scrub Lagoon but also reach Scrub Lagoon from the other side of the island through a low topographic path. The intra-arc (F1, F2… F14), intra-slab (IS1, IS2), ridge (R1, R2), wedge (W1, W2, W3) and deep inter-plate (IT1, IT2) provide wave height too small to pass the topographic threshold (Figure 9) and to reach tsunami sediment records, as shown on Figure 10 (medium blue color in histogram b) with very low correlation coefficients for Anguilla and Scrub.

b) Analysis of simulation results on Anegada Island

The tsunami simulations on Anegada were performed on a 5 m resolution grid with synthetic record of the waves on four locations along the north coastline (Ane1, Ane2, Ane3, Ane4 mapped on Figure 9). The results for the maximal water heights recorded along the coast, at each location, generated by the 11 selected fault models are presented in Figure 9.

Almost all the mega-thrust and outer-rise models generate waves high-enough to produce run-ups reaching some deposits locations (T1, T2, T3, T4 and OR1, OR2, OR3 and OR4 in Figure 9). The outer-rise faults OR1, OR2 and OR3 located just in front of Anegada generate waves reaching 5 to 13 m (Figure 9b) that largely exceed the topographic threshold at most of the locations. Except for the easternmost models OR4 and OR5 that generate much smaller waves, the correlation coefficients (histogram b, Figure 10) are among the highest. The extent of the flood obtained with fault OR3 on Anegada is shown in Figure 12, the run-up reaches almost all deposit locations expect for the most remote one on land and on the south-west coast of the island. Similarly, the four mega thrust models (T1, T2, T3, T4) generate waves that reach at least 3 m to 4 m and up to 10 m for models T1 and T2. They largely exceed the topographic thresholds (Figure 9a), even the model T4 that is the further trench segment from Anegada. Figure 11 shows the large run-up generated by fault T2, the tsunami floods the entire island expect for the highest reliefs and reaches all deposit location. The consistency of these mega-thrust simulation leads to correlation coefficients close to 1 (histogram b, Figure 10). The intra-arc (F1, F2… F14), intra-slab (IS1, IS2), ridge (R1, R2), wedge (W1, W2, W3) and deep inter-plate (IT1, IT2) fault models generate maximal waves of 0 to 2 m and remain lower than the topographic threshold of 2 to 4 m which result in low correlation coefficients are low as well (histogram b, Figure 10).

c) Analysis of simulation results on Saint-Thomas

The tsunami simulations on the area of Saint-Thomas were performed on a 10 m-resolution grid with synthetic wave records at 6 tsunami deposits locations (mapped on Figure 6). The

results for the maximal water heights recorded along the coast generated by the 11 selected fault models are presented in Figure 9. The correlation coefficients for Saint-Thomas are indicated in light blue in the histogram b in Figure 10.

Only the mega-thrust and outer-rise models generate waves high enough to run-up and reach some deposit locations (T1, T2, T3, OR1, OR2, OR3 and OR4 in Figure 9). The outer-rise models OR1, OR2, OR3 and OR4 generate wave heights of 1 to 4 m (Figure 9b) and, except for OR5, result in high correlation coefficients (Histogram b in Figure 10). As shown in Figure 12, OR3 tsunami floods the four ponds of Salt Cay, Saba Pond, Magen Bay and Cabrita Pond where sediments were cored. The most northern segments of the trench, T1 T2 and T3 generate consequent wave heights of 2 to 8 m at the coast (Figure 9a) and result in high correlation coefficients (Histogram b in Figure 10). As shown in Figure 11, T2 tsunami floods the four ponds of Salt Cay, Saba Pond and Magen Bay. Among the rest of the models, only the interplate model IT1 produces important waves and run-up in the five lagoons and could be consider as other candidates for these deposits as shown on the histograms of Figure 10.

d) Tsunami intensity and inundation

In order to better compare the results of outer-rise and mega-thrust models, we extracted from the simulation, wave height and velocity profiles along two sections of Anegada island and two sections of Scrub Island (Figure 13). The results obtained for the trench models T1, T2 and the outer-rise models OR1, OR2, OR4, and OR5. This figure is inspired by Buckley et al. (2012) who also performed and compared tsunami simulations on Anegada island with several fault scenari.

The mega-thrust models T1 and T2 largely flood both islands, Anegda and Scrub, with wave reaching all deposits position as shown in the four profiles (XX', YY', WW', ZZ'). In Anegada, all the outer-rise models reach the deposits on the XX' profile but only model OR1 (green line) reaches the most central deposit on the YY' profile. However, in Scrub WW', if all the outer-

rise models overpass the barrier, only model OR4 generate significant wave heights at the core position. In Scrub Lagoon, the flow thicknesses of the outer-rise models are smaller than 1 m and very small compared to the values of 3 m to 6 m obtained with the mega-thrust models T1 and T2 which are more convincing for transporting sediments. In addition, the very high wave heights and flow thickness of the mega-thrust models leave room for testing faults rupture of smaller magnitude with smaller slip or size. On contrary, the simulated outer-rise tsunamis seem slightly too weak to explain all observed deposits, it might be corrected by increasing the fault size or the slip intensity but leading to unrealistic fault models since they are already exaggerated beyond all existing similar events in the literature.

In Buckley et al. (2012), they compare the waves generated by a Mw8.7 mega-thrust model, a Mw8.0 outer-rise model, a 1755 Lisbon fault model and a storm. Their mega-thrust model generates much smaller waves than ours because they use a source of 630 km length (T1 and T2 length is 200 km) with a slip of 8.6 m (T1 and T2 slip is 20 m) leading to a tsunami energy that is spread over a larger area. Using sediment transport inverse modeling, they calculate the minimum wave velocities required for the transport of the observed sediments. Only their outer-rise model generates consistent velocities for the sediment transport while both our mega-thrust and outer-rise models generate consistent velocities with equivalent and higher values.

d) General analysis

Considering the simulation's results on each island independently, it enables us to identify which scenarii could be compatible with each group of tsunami deposits separately. Among all the models, only the subduction thrust faults and the outer-rise faults are able to generate tsunamis waves high enough to reach the deposit location whether in Anegada, Saint-Thomas or Anguilla. The ridge models (R1, R2), wedge models (W1, W2) and interplate model IT1 generate significant wave heights in Saint-Thomas and Anegada islands but they

just reach the topographic threshold and barely flood the coast and the ponds. Sources of this kind could be considered as a good candidate for some of the identified deposits only if they were increased in size or slip intensity.

Among the 9 models (T1, T2, T3, T4, OR1, OR2, OR3, OR4, OR5) compatible with part of the deposits in the three considered islands, only the thrust model T2 tsunami generated wave heights above the coastline threshold at all locations (highest correlation coefficient in histogram a of Figure 10). The inundation limits of the best model T2 (Figure 11) are very coherent with the deposit's distribution, especially in Anegada. All the other models only fit one or two of the islands, T1 for example waves barely affect Anguilla Long Pond, the outer-rise OR1, OR2 and OR3 barely flood Anguilla Long Pond and Scrub lagoon.

The mega-thrust models are not discussed there because they generate a tsunami very similar to T2 and T3 models but with surprisingly slightly smaller waves. The slip intensities for the mega-thrust models are 20 m (MT1 and MT2) and 30 m (MT1b and MT2b), it is equivalent or greater than 20 m slip used for the thrust models (T1, T2, T3, T4). In addition, the rupture occurs on a wider area of 300*100 km for mega-thrust so the resulting magnitudes (Mw8.8 and Mw8.9) are greater than the thrust models (Mw8.7). However, the results of the simulations indicate equivalent or smaller wave heights in the near field. This could be explained by a phenomenon of wave energy concentration toward smaller areas; the energy from a smaller source will be directed toward a more constrained area while the energy from larger sources spread on a wider area will result in equivalent waves at near-field coasts. If the differences between those sources is not evident in near-field, it clearly appears in far-field. Indeed, the mega-thrust simulations show greater tsunami amplitudes towards the Bahamas, Florida and Canadian coasts in comparison to the amplitudes generated by the thrust models.

f) **Far-field simulations**

A set of far-field tsunami simulations were performed on a 500 m-resolution grid of 600*1000 km that encompasses all the Caribbean Sea and its coasts, the Northern coast of Venezuela, the Greater Antilles, the coasts of Florida and the Bermudes (Figure 14). Another set were performed on a 2 km resolution grid covering an even greater area up to the European coasts (Figure 15). Time series of the modelled tsunami were recorded in Puerto-Rico, Jamaica, Bonaire, Aruba and Curaçao (Figure 14), the locations where deposits of the same age have also been identified (Figure 3). Time series of additional locations (Barbados, Bermuda, Florida) are also presented (Figure 14). Only the best fitting scenarii from the near-field study were far-field simulated, it corresponds to the fault models T2, MT1, MT1b, MT2 and MT2b, and here we present the results for the model MT1.

The resolution of our grid only allows an estimation of the wave amplitude offshore and the gages are located 5 km to 10 km offshore the coast. The amplification of the tsunami waves generally occurs in the last hundred meters before the coastline, where the water depth rapidly decreases and consequently the wave amplitude rapidly increases. The factor of amplification varies depending on the sites, but it can be of 2 to 5 between a low resolution grid and a fine grid. The Green's law (Green, 1837) can be used to calculate an estimation of the height at the coast (H_{coast}) from the height recorded offshore (Hsea), the depth offshore (Dsea) and the depth at the coast (Dcoast) which is considered at an average value of 2 m:

$$H_{coast} = H_{sea}\left(\frac{D_{sea}}{D_{coast}}\right)^{\frac{1}{4}}$$

The factor of amplification $(D_{sea}/D_{coast})^{1/4}$ has been calculated at each gage location and applied to the associated signals in Figure 11 (original signal in black and estimated amplified signal in red). In Puerto-Rico the factor equals 1.37 giving an amplified height of 1.37 m. In Culebra the factor equals 1.01 giving an amplified height of 3.5 m. In Jamaica the factor equals to 1.41 giving an amplified height of 0.35 m. In Aruba the factor equals 2.03 giving an

amplified height of 1.62 m. In Curaçao the factor equals 2.53 giving an amplified height of 3.80 m. In Bonaire the factor equals 2.10 giving an amplified height of 2.3 m. In Florida the factor equals 1.68 giving an amplified height of 0.84 m. In Bermuda the factor equals 4.07 giving an amplified height of 8.54 m. The values of depth are extracted from the 500 m resolution grid and might be different from reality leading to an inexact amplification factor. So, these estimations of height give an idea of the potential gap between the values offshore and along the coast, but they should be considered carefully.

The maximal waves generated in the area of Puerto-Rico and Culebra Islands range between 1 and 4 meters and probably even more in finer grids. They are high enough to pass the sandy barriers of 2-3 m high separating a pond in Culebra Island (Donnelly et al., 2005) from the sea, a pond where sediments deposited soon after the period 1100-1300 cal yr CE were identified. The maximal wave heights generated along the coast of Jamaica are around 0.5 m that might be amplified to 1 or 2 m in finer grids. Those values are just high-enough to reach the deposits identified in a lagoon that are separated from the sea by barriers of 1 to 4 m-high (Palmer et al., 2020). In Aruba, Bonaire and Curacao the highest waves reach between 1 and 5 meters, and might also be amplified in finer grids, these values are again just enough to reach most of the tsunami deposits identified on those islands located between 0 and 5 m above sea level (Engel et al., 2016). All these far-field waves seem to be just high enough to generate flooding at the deposits locations so we cannot affirm that they could generate the transport the observed sediments, but we cannot deny it either. Indeed, those values are rough estimations so higher resolution simulation should be done in order to draw conclusions concerning the potential link between those far-field deposits and the Antilles deposits.

The far-field simulations are also useful to identify areas where local wave amplification can occur. The maximum elevation maps show that wave amplification occurs for Bermudes Islands, the northern part of the Bahamas and Florida Coast. For sources located on the northern segment of the Lesser Antilles Arc, the energy is focused partly toward the

Bermudes where the waves reach maximal amplitudes of 8 m after amplification on the Southern coast. However, until now the analysis of sediments along the coasts of Bermuda Island do not show tsunami deposits (Ellison et al., 1993; McMurty et al., 2007; Hengstum et al., 2014; Wallace et al., 2017; Kemp et al., 2019). Only a study of coral growth (Drascba et al., 2000) indicates some unexplained stops in the growth curve at an age around 1400-1450 cal yrs CE.

Some tsunami waves also present important amplitudes toward the coasts of Florida and Bahamas Islands with heights reaching 1 to 2 meters (in the maximal water height map) and surely more in finer grids. In the USA, two major overwash deposits dating of 1319–1351 cal yrs CE and 1428–1492 cal yrs CE have been identified in several places along the coasts of New Jersey, Rhode Island and in Connecticut (Donnelly et al., 2001b; Donnelly and Webb, 2004; Nikitina et al., 2015). Bahamas islands are also intensively studied for the hurricane activity, and extreme event deposits dating from ~ 1500 cal yr CE were identified in Eleuthera, Long Islands, Long Islands Blue Hole and Blackwood Sinkhole (Kettelat et al., 2004; Wallace and Donnelly, 2021; Winkler et al., 2020; VanHengstum et al., 2016). They are constituted of heavy boulders, thick surface sand layers and overwash layers in sediment cores. The hypothesis that some of these deposits could be related to an Antilles earthquake generated tsunami is not impossible.

VI – Discussion

a) Simulation uncertainties

Tsunami simulations lay on two main inputs, which are the source and the bathymetry. The simplification of the seismic source by a homogeneous Okada model remains generally as a good approximation of major events with unknown mechanisms, even more so when there is no recording but only rough estimates of wave impacts and heights. The bathymetry and topography are also sources of uncertainty, because they possibly evolved during the past,

here the last 500 years.

First, if an earthquake occurs close enough to the islands, they can be affected by the coseismic deformation associated with the rupture. From the studies of corals and the coastal morphology of these northern Lesser Antilles islands, no evidence of brutal subsidence or uplift has been identified yet. This absence can be used for constraining the rupture area of a potential past earthquake. The areas of coseismic deformation associated with our mega-thrust and outer-rise models do not reach the islands which is consistent with this absence of deformation.

Only a long-term tectonic subsidence of the Lesser Antilles of 0.5 to 2 mm/yr has been recently identified and calculated from micro-atoll data (Weill-Accardo et al., 2016), from reef terraces (Leclerc et al., 2014, 2015) and from modern geodetic data (van Rijsingen et al., 2021). This subsidence and the impact of past extreme waves might have transformed the coastline over the years. For example, the sandy barriers on Anegada northern coast or in Scrub and Anguilla might have been lower than now or might have not existed in Pre-Colombian times. Without them, the waves generated by the outer-rise models would become more threatening and these scenarios more consistent. On the contrary, if these topographic heights were even higher than now, some of our models would become less convincing.

The lack of knowledge on the Pre-Columbian islands environment generates additional uncertainties when selecting a Manning coefficient value for the simulation. It is a fixed parameter that expresses the friction of the water on the floor and can be chosen depending on the nature of the ground. In the literature, this coefficient values range between 0.01 for water area to 0.2 for high density urban area (Kaiser et al., 2011; Bricker et al., 2015). The exact values for each type of land vary depending on the used code and models. For TAITOKO and for the Antilles islands that show small coastal reliefs and a heathland vegetation, we chose a Manning coefficient value of 0.02. But depending on the vegetation

and coastal morphology in Pre-Columbian times, this coefficient could be re-evaluated which would impact the simulation results.

The last source of uncertainties presented here, is the long-term conservation of the sediments deposits. Indeed, Spiske et al. (2018; 2020) show how important the erosion of sediments caused by weather and bioturbation is. Boulders can be moved and re-shaped by the waves and wind, bioturbation can destroyed the sedimentary structures of the deposits and even lead to their total erosion. This is the reason why the absence of deposits is never considered as evidence of a past inexistent or low wave impact. For this same reason, the thickness of these deposits cannot be used as an argument of wave intensity even more knowing the complexity of the deposition processes as detailed in the next paragraph.

b) Tsunami intensity and sediment transport

Some major studies of the tsunami sand deposits associated with the most recent tsunamis like in 2015 and 2010 in Chili (Morton et al. 2011, Bahlburg et al., 2013), in 2011 in Tohoku (Namegaya and Satake, 2014) or in 2004 in Sumatra (Paris et al., 2009, 2010; Lavigne et al., 2009) report values for sediment distribution and thickness where real observations or records of coastal water heights, flow depths and flow velocities have been done. Most of the studies highlight the wide range of sediment thickness identified over the inundation areas and the complexity of sediment transport processes that depend on the topography, nature and availability of the sediments, wave dynamics and many other factors.

One aspect noticed by sedimentologists is the gap between the water run-up boundary and the sediment run-up boundary after a given tsunami. In Sendai Bay, the 2011 Tohoku sediment run-up distance corresponds in average to 60-70% of the total tsunami run-up distance (Abe et al., 2012; 2020; Chague-Goff et al., 2012; Sawai et al., 2012; Fujiwara et al., 2020), in some places affected by the 2010 Chile tsunami the sediment run-up distances are approximately 70- 80% of the tsunami run-up distances (Morton et al., 2011). But in other deposits sites, the sediment run-up distance reaches up to 90%-100% of the tsunami run-up

distance like in the Kuril Islands after the 2006/2007 tsunamis (MacInnes et al., 2016), in the Galapagos Island after the 2011 Tohoku tsunami (Arkos et al., 2013), in New Zealand after the 2016 Kaikoura earthquake (William et al., 2018) or in Banda Aceh after the 2004 Sumatra tsunami (Lavigne et al., 2009; Paris et al., 2009, 2010). The analysis of the configuration of these different places shows that the gap between deposit boundary and inundation limit might increase with the flatness of the land. This gap is the greatest in Sendai Bay which consists of a 3 to 4 km-long smooth and flat slope (slope of 0.05%) where deposition limit stops at 3 km when water reaches distances of 4 km inland (Namegaya et al., 2014). In Chile, La Trinchera site shows a 150 to 200 m gap, it corresponds to a deposition distance 80% of the inundation distance on a very smooth and flat land (slope of 0.7%) without any topographic features. By contrast, the presence of steep topographic features might stop the flood before the end of the deposition processes and prevent the apparition of this gap. For example, in Banda Aceh, both the limits of deposition and inundation correspond to the presence of reliefs and that is the case of many of other sites like in the Galapagos, in New Zealand or in Hawaii where the coastal topography is steep.

In the studied sites of the Lesser Antilles islands, the coasts do not present smooth and flat slopes but either relatively steep and high reliefs. The northern coast of Anegada is characterized by 2 to 5 m-high sediment barriers along the coastline and flat lowlands in the backshore where most of the deposits are located (Figure 5). In Saint Thomas, the deposits have been found on lagoons and ponds surrounded by reliefs with steep slopes (20% in Salt Cay, 10% in Magens Bay, 10% in Smith Pond, 20-30% in Cabrita Pond and Saba Pond) that rapidly exceed heights of 10 m and that likely stops a tsunami wave (Figure 6). In Anguilla, the coastline corresponds to a succession of steep slopes (5% in the south and 30-40% in the north) (Figure 4). Long Pond and Scrub Lagoon are isolated from the sea by a 3 to 4 m-high sediment barrier and are surrounded by rocky reliefs onshore. Thus, on the high plateau of Anegada or Anguilla and Scrub Islands the water inundation limit might have reached greater distance than the reported deposition locations. However, in the coastal lagoons of Anguilla,

Scrub and Saint Thomas the inundation distances probably correspond to the deposition distances. Given the geomorphological characteristics of the study sites, it is likely that sediment records are indicators of minimal values of inundation limits. A more detailed evaluation of the wave heights, shapes and intensities necessary for sediment transport is a complex topic that is not well defined yet (Cox et al., 2019).

c) Rupture of the subduction contact and the coupling debate

The hypothesis of a rupture along the subduction interface is joining the list of the two mega-thrust rupture hypotheses associated to the 1843 and 1839 events. However, except for these two debated events, no rupture of the Lesser Antilles subduction zone for the last 500 yrs has been demonstrated. In the case where the earthquakes of 1843, 1839 and the potential Pre-Columbian event were actually interplate ruptures, since then the faults should have relocked because this process is considered stable over thousands of years by recent models of seismogenic behavior in subduction zone (Avouac 2015; Mouslopoulou et al., 2016; Jolivet et al., 2020). Our subduction fault models are distributed on two plates separated by the Anegada Passage: the Puerto-Rico micro-plate and the Caribbean plate that are modeled separately in geodetic analysis.

The Puerto-Rico trench presents a very small slip deficit that indicates that the interface is likely uncoupled. A deep interseismic coupling is suspected in Hispaniola, north of Puerto-Rico, with transition from coupled to uncoupled plate interface for Hispaniola to Puerto-Rico that coincides with the existent fault systems in this area (Symithe et al., 2015).

For the Lesser Antilles, geodetic (GNSS) and microatoll datasets both indicate a general subsidence of the arc which can be interpreted in favor or disfavor of a locked interface depending on the used interseismic coupling model. The geodetic studies indicate an actual very low, almost nonexistent coupling of the subduction contact (Manaker et al., 2008; Symithe et al., 2015; van Rijsingen et al., 2020). They measure over the past 20 years a

general subsidence of the Lesser Antilles of 1-2 mm/yr that they interpret as a consequence of long-term geodynamic processes associated to the aseismic character of the subduction (van Rijsingen et al., 2021). The deformation map produced by their interseismic coupling model, which corresponds to a shallow coupling, indicates an uplift of the islands inconsistent with the measured subsidence. In contrary to these results, the interseismic coupling model used in the microatoll study (Philibosian et al., 2022), which correspond to a deep coupling, results in the subsidence of the arc consistent with the 8 mm/yr measured from the corals. The contradictory results from these two studies comes from the shallowness of the used coupling model. But it could also come from the difference of period covered by the datasets,100 years for the microatolls and 20 years for the GNSS, which might indicate a variation of the coupling over the past century (Philibosian et al., 2022). It is also possible that GPS measurements are missing a part of the slip and even if this interface was partially coupled, Symithe et al. (2015) estimates from the geodetic data that it would lead to an event of magnitude Mw>8 to occur only every 2000 or 3000 years. In this case the occurrence of three mega-thrust earthquakes (in Pre-Columbian times, in 1843 and in 1839) would require again a change of the coupling state over the past centuries. Finally, the coupling of the Lesser Antilles is still debated but the hypothesis of a mega-thrust Pre-Columbian earthquake is realistic and compatible with some of the models.

A similar problem has been issued in the study of the 1957 Andreanof Islands Mw8.6 earthquake that generated a large tsunami in the Aleutian Islands. The results of tsunami simulations (Witter et al., 2016, 2019) compared to the deposits observed on the islands imply a megathrust slip in an area where geodetic coupling models indicate the opposite.

d) The storm hypothesis

Past storms can be considered as a strong alternative hypothesis to the earthquake one. Indeed, the Lesser Antilles is a region impacted by tropical storms and hurricanes which regularly strike and damage those islands (Andrews, 2017; Krien et al., 2017; Biguenet et al.,

2021). The hurricane activity in the region during the last millennium is divided in two periods of interest (Biguenet et al., 2021). A period with a high frequency of hurricanes in 1080-1230 cal yrs CE probably linked to the Medieval Warm Period (800-1300 cal yrs CE) and a period without hurricanes in 1400-1600 cal yrs CE probably linked to the beginning of the Little Ice Age (1450-1900 cal yrs CE). The Pre-Colombian deposits are dated between 1200 cal yrs CE and 1600 cal yrs CE in a period of low frequency hurricanes and no exeptionaly strong hurricane from that period was identified in other sediment records of the region, which does not mean that it did not occur.

Storm and tsunami deposits are still difficult to discriminate against. Sedimentologists who analyzed the sediments and cores in Anguilla, Scrub and Saint-Thomas favor the tsunami hypothesis but they do not exclude the storms hypothesis. In Anegada, one point for this discrimination could be the presence of the enormous coral boulders in the heights of the island, whose sizes make the scenario of a storm less convincing than a tsunami. Even the strongest hurricanes of the past centuries the Great Hurricane in 1780 (category 5), Dona in 1960 (category 4) or Irma in 2017 (category 5) did not transported such large sand deposits or boulders on the coasts of the islands (Spiske et al., 2021). However, one or several exceptionally damaging hurricanes still might have strike the Lesser Antilles during these Pre-Columbian times.

The only known storm having transported an amount of sediments similar to the Antilles Pre-Columbian one is the 2013 super typhoon Haiyan. It generated waves of 8 m and transported hundreds to thousand massive boulders (up to 30 tons) in Calicoan Island in the Philippines (Kennedy et al., 2016). Another Super-Typhoon, Soudelor in 2015, generated waves of 12 m in Taiwan transported massive amount of sand and a boulder of 1.4 m diameter onland (Huang et al., 2020). Many other super-typhoons of the same intensity have occurred on this region in the past : Tip in 1979, Bess in 1982, Megi in 2010. The absence of field survey on the coastal impacts of these past events do not allow to conclude on the capacity of their associated waves to transport sediments. However, instrumental records indicate that the

storm wave heights of past typhoons often range between 9 to 11 m in Taiwan (Huang et al., 2020). So only for the 50 past years there are several examples of massive boulders and sediment transported by storms in the West Pacific region while there is no such observation in the north of the Lesser Antilles for the past 500 years. Unless such events did not leave any traces anywhere or that their traces were completely eroded, it indicates that an event capable of transporting Anegada's boulder and the other island sediment deposits must be very rare, exceptional.

e) The landslide hypothesis

Landslide-generated tsunamis are known to be as dangerous as earthquake-generated tsunamis, and can be triggered by volcanoes, earthquakes or storms: phenomena that can occur in the Lesser Antilles arc. During the CASEIS cruise in 2016 (DOI:10.17600/16001800), paleo-seismological investigations were carried out in the forearc basin of the northern segment of the arc between Anegada and Barbuda at depth between 5200 and 5800 m. From 7 cores, 3 megadeposits (homogenite-turbidite complexes HmTu) older than 8ka BP were identified as being possibly generated by major tsunamis but nothing around 1500 cal yrs CE (Morena et al., 2019). Seismic profiles and bathymetry did not reveal any fan or traces that could be associated with a major landslide in the area. Similar studies were carried out in the east part of the Virgin Islands and Whiting basins where no evidence of recent sediment transport was detected, the youngest turbidite dating from ~2000 years ago (Chaytor et al., 2015). Moreover, landslide generated tsunamis generally show locally important amplitudes that rapidly decrease with distance from the source. In this case, where deposits of the same age are spread over an area of 100 km2, a landslide could be associated with one of the three island deposits but could not explain them all. The absence of turbidite dating from the Pre-Columbian period could be in disfavor of the single tsunamigenic earthquake hypothesis but the processes associated to the generation of turbidites are complex. Turbidity currents can be triggered only if the conditions (the bathymetry, the sediment load, the flow

dynamics…) are reunited and can result in discontinuous deposits (Ge et al. 2022), which justify this absence of such deposits dating from Pre-Colombian period even if a large tsunamigenic earthquake occurred at that time.

f) Multiple intermediate events or one extreme event?

With the premise that all the Pre-Colombian deposits correspond to one same event, the general analysis of the tsunami amplitudes shows that only a subduction thrust rupture model gives good fitting results for all deposit location at once. An outer-rise rupture could become an equally convincing scenario with perhaps a different parameterization. The hypothesis of one unique event is then plausible and can explain the presence of these synchronous deposits. However, considering the uncertainties in the ages of these deposits, all or part of them being unrelated is a possibility which would imply that they were generated by several concomitant events.

The independent analysis of the tsunami amplitudes generated at each of the three sites show that several Outer-Rise fault ruptures are possible candidates to explain the Anegada's deposits and Saint-Thomas's ones. An intraplate fault rupture also appears as a potential candidate for Anegada Island and also for Anguilla and Saint-Thomas with a different location and orientation. Even if these scenarios are smaller the single mega-thrust one, they still are Mw 7.5-8 exceptionally great unprecedented events in the area. So this hypothesis implies that at least two or three of these major earthquakes and tsunamis at the origin of Anegada, Anguilla and Saint-Thomas's deposits, were generated at the same period of time in this region.

The range of 300 to 500 years given by the deposit's chronologies (1200-1500 cal yrs CE with uncertainties) is large enough to consider the occurrence of several major earthquakes or storms. Based on the historical catalog only one tsunami of this magnitude occurred in all the Lesser Antilles during the last 300 years: the 1867 tsunami of the Virgin Islands. The probability of 2 or 3 Magnitude 7.5-8 tsunamigenic earthquakes occurring in this small area in

the same period of time seems quite low. At the same time, the probability of a single Magnitude 8-9 class mega-thrust or outer-rise earthquake is quite low as well. And if we consider the storm, the reflection is the same, there is no evidence of such amount of sediment transported by past storms in this area. So, the probability of several exceptionally strong hurricanes occurring during this 300 to 500 years period seems quite low as well.

Since these occurrence probabilities are not quantified in this paper, it is difficult to draw a definitive conclusion but the scenario of one single event, be it an earthquake or a storm, remains more convincing following the logic of Ockham's razor.

g) A major earthquake or a major storm: far-field impact

With this study, we considered that we have not omitted any earthquake generated tsunami scenario. All the results from the tsunami simulations converge toward the mega-thrust models that generate flooding areas very coherent with the sediment deposits, especially for the T2 model facing Anegada Island. This T2 Mw8.7 mega-thrust model present a maximized slip value of 20 m but it would be interesting to test the same model with smaller slip values of 15 m (Mw 8.6) or 10 m (Mw 8.5) to identify the slip and magnitude values thresholds for compatible scenario. The results also highlight the outer-rise models consistency which should be studied further in order to deduce their capacity to generate the observed deposits. The small number of similar historical events makes the choice of fault parameters difficult and uncertain, in our model the values of size and slip are constrained by these of the greatest pre-existing events but we should consider modeling even greater outer-rise ruptures since the fault traces are particularly well defined in this area. The analysis of seismic profiles of the trench could provide more information about the dimensions of these faults. In the Lesser Antilles, the occurrence of such Mw>8.0 outer-rise earthquake would be as exceptional as the occurrence of a Mw>8.5 mega-thrust earthquake.

The occurrence of a great hurricane is the other possibility mostly supported by the great sediment transport associated to the Super Typhoon Haiyan. The boulders and deposits

identified in the ABC islands south of the Lesser Antilles (Aruba, Bonaire and Curaçao) which are attributed to waves generated by one or several past storms (Scheffers et al., 2002; Radtke et al., 2003; Morton et al., 2006; Engel et al., 2016), are also evidences that extreme storms can occur in the region. However, a hurricane passing on the south of the Lesser Antilles might have a different impact than a hurricane passing on the north of the arc with, and the differences of island morphology also influence the storm surges. It should be shown that such an event could produce floods on Anegada, Scrub, Anguilla and Saint-Thomas as coherent with the observations as obtained with the earthquake-generated tsunami. In addition, some of the sediment deposits are clearly identify as resulting from a tsunami (Biguenet et al., 2021) and disfavor the storm hypothesis.

One way to answer the question of the deposits origins and to discriminate the earthquake and storm hypotheses, could rely on the study of the shape and wideness of the region impacted. Storm surges can be produced locally wherever the hurricane passes resulting in a large area of impact but limited to the shape of the hurricane pathway. While a tsunami generated by an earthquake can propagate at very far-field and impact trans-oceanic regions, as it has been observed for the 1755 Lisbon tsunami or the 2004 Sumatra tsunami.

Indeed, as shown in Figure 15, a major earthquake occurring on the north of the Antilles arc generates trans-oceanic waves that propagate through the Atlantic towards North America and Europe. Those waves are modeled with a 500 m grid resolution and might be two to five times higher in grids of finer resolution. The wave amplitudes along the northern coasts of the USA do not exceed 1 m while they exceed 2 m along the Canadian coasts (New Scotland). These localized amplifications are strongly related to the orientation of the source and can vary depending on the modeled scenario. The most impacted place seems to be the Bermuda Islands, where 5 to 10 m wave heights are simulated on their southern coasts but where no traces of tsunami were identified yet. In Canada as well, no overwash deposit dating from approximately 1500 cal yr CE has been reported yet. The presence of such deposits in Bermuda Islands and in Canada would be a strong argument in favor of the tsunami

hypothesis. The modeled tsunami waves also reach Europe but with smaller amplitudes that do not exceed 1 m. Some amplification phenomena are occurring offshore Ireland and England with 1 to 2 m waves. A more detailed study on the far-field impacts should be done with finer grids and with the use of Boussinesq Equation more adapted to such deep water environments like the Atlantic Ocean.

The current absence of deposits along the Atlantic coasts that could be associated to a trans-atlantic tsunami originated in the Lesser Antilles is the only argument in disfavor of the hypothesis of a major Pre-Columbian earthquake. However, this absence can be explained by the age of the event with deposits that might be buried too deeply to be recovered, by the disappearance or erosion of the deposits if they were too small, and by the lack of field surveys in the areas of interest.

Conclusion

Tsunami simulations were performed on high-resolution grids of the Northern segment of the Lesser Antilles arc and compared to the ~500yrs old tsunami deposits reported in the literature. Among the 35 fault models tested, only some magnitude Mw>8 mega-thrust and outer-rise earthquake models generate a tsunami high-enough to explain the presence of the deposits identified on the islands of Anguilla (Scrub), Anegada and Saint-Thomas. Several other models generate significant tsunami waves along the coast but are not high-enough to reach deposit locations with a realistic sediment transport potential. The results show that the event must have reached extreme magnitudes regardless of the involved fault system. They also show that localized distinct tsunamis on each of these islands must still be generated by Mw>7 earthquakes which enlarge the list of potential sources but does not solve their identification.

Due to the very complex tectonic nature of this subduction zone, high-magnitude intraplate

earthquakes at 30 to 50 km could be a hypothesis but they imply important rupture depths leading to significant attenuation for tsunami generation, which is not compatible with the observed deposits heights. Outer-rise fault models generate large wave heights that could match all the deposits location in all islands only with increased fault dimensions or slip intensity. From the tsunami modeling perspective, one or several tsunamigenic earthquakes of Mw 7.5-8 could have produced these deposits but at least one of them must have been an outer-rise earthquake of Mw 8.0 or a mega-thrust earthquake of Mw 8.5-9.

The occurrence of a mega-thrust earthquake on this subduction interface is debated due its uncertain coupling. However, important turbidite deposits on deep forearc basins of the Lesser Antilles, with recurrence time of several thousand years have been identified (Seibert et al., 2019). They could indicate that this subduction interface is characterized by a very long seismic cycle which would mean that no mega-thrust earthquake is expected before a thousand years in this region of the arc.

Finally, the occurrence of one or several strong hurricanes cannot be excluded but there is no strong evidence in favor of this hypothesis. Adding sediment transport models to the simulation of the tsunami would bring new constraints on the tsunami waves (size, velocity, number…) and on the source. Boulders on Anegada could be particularly useful in determining a threshold for a minimal wave height and a minimal magnitude for this event. And, the identification of tsunami deposits at far-field locations especially in Bermuda and along the Canadian coasts would drastically strengthen the credibility on the occurrence of one or several Pre-Columbian earthquakes and would give a better idea on the impact extent of the tsunami. So new field surveys and field data from all around the Caribbean Sea and the Atlantic are still needed for validating all these models.

Acknowledgments

This study was supported financially by the ANR CARQUAKES (contract number

ANR-17-CE3-0006), the Interreg Caraïbes PREST, FEDER European Community (program number CCI 2014TC16RFTN008) and the Commissariat à l'énergie Atomique (CEA). We thank the different agencies who provided the bathymetric and topographic dataset: NOAA, SHOM, IHO, BODC, IOC, UNESCO and USGS. The work is based on the analysis of data published in previous papers and the code TAITOKO used to make the tsunami models belongs to CEA and is not available publicly. We especially thank Brian Atwater and Michaela Spiske for reading and fruitful discussions. We also thank one anonymous reviewer for reviewing the manuscript and giving constructive comments that helped improving the article. This is an IPGP contribution number XXXX

References

- Abe T., Kazuhisa Goto, Daisuke Sugawara, Relationship between the maximum extent of tsunami sand and the inundation limit of the 2011 Tohoku-oki tsunami on the Sendai Plain, Japan, Sedimentary Geology, Volume 282, 2012, Pages 142-150, ISSN 0037-0738, https://doi.org/10.1016/j.sedgeo.2012.05.004.

- Abe, T., Goto, K. & Sugawara, D. Spatial distribution and sources of tsunami deposits in a narrow valley setting - insight from 2011 Tohoku-oki tsunami deposits in northeastern Japan. Prog Earth Planet Sci 7, 7 (2020). https://doi.org/10.1186/s40645-019-0318-6

- Ammon, C., Kanamori, H. & Lay, T. A great earthquake doublet and seismic stress transfer cycle in the central Kuril islands. Nature 451, 561–565 (2008). https://doi.org/10.1038/nature06521

- Andrews B.D., Ten Brink U.S., Danforth W.W., Chaytor J.D., Granja Bruña J.L., Llanes Estrada P., et al., Bathymetric Terrain Model of the Puerto Rico Trench and the Northeastern Caribbean Region for Marine Geological Investigations. Retrieved from. https://pubs.usgs.gov/of/2013/1125/. (2013)

- Andrews, Alexa Jo, "Spatial and temporal variability of tropical storm and hurricane strikes in

the Bahamas, and the Greater and LesserAntilles" (2007).LSU Master's Theses. 3558.https://digitalcommons.lsu.edu/gradschool_theses/3558

- Anglade, A., Lemarchand, A., Saurel, J.-M., Clouard, V., Bouin, M.-P., De Chabalier, J.-B., Tait, S., Brunet, C., Nercessian, A., Beauducel, F., Robertson, R., Lynch, L., Higgins, M., & Latchman, J. (2015). Significant technical advances in broadband seismic stations in the Lesser Antilles. Advances in Geosciences, 40, 43–50. https://doi.org/10.5194/ADGEO-40-43-2015

- Atwater B.F., ten Brink U.S., Buckley M., Halley R.S., Jaffe B.E., López-Venegas A.M., Reinhardt E.G., Tuttle M.P., Watt S., Wei Y. Geomorphic and stratigraphic evidence for an unusual tsunami or storm a few centuries ago at Anegada, British Virgin Islands. Natural Hazards 63, 51–84. https://doi.org/10.1007/s11069-012-9622-6 (2012)

- Atwater B.F., ten Brink U.S., Cescon A.L., Feuillet N., Fuentes Z., Halley R.B., Nuñez C., Reinhardt E.G., Roger J.H., Sawai Y., Spiske M., Tuttle M.P., Wei Y., Weil-Accardo J., 2017. Extreme waves in the British Virgin Islands during the last centuries before 1500 CE. Geosphere 13, 301–368. https://doi.org/10.1130/GES01356.1

- Arcos, M., MacInnes, B., Arreaga, P., Rivera-Hernandez, F., Weiss, R., & Lynett, P. (2013). An amalgamated meter-thick sedimentary package enabled by the 2011 Tohoku tsunami in El Garrapatero, Galapagos Islands. Quaternary Research, 80(1), 9-19. doi:10.1016/j.yqres.2013.04.005

- Avouac, JP., Meng, L., Wei, S. et al. Lower edge of locked Main Himalayan Thrust unzipped by the 2015 Gorkha earthquake. Nature Geosci 8, 708–711 (2015). https://doi.org/10.1038/ngeo2518

- Baillard C., Wayne C. Crawford, Valérie Ballu, Bernard Pelletier, Esline Garaebiti; Tracking subducted ridges through intermediate-depth seismicity in the Vanuatu subduction zone. Geology 2018;; 46 (9): 767–770. doi: https://doi.org/10.1130/G45010.1

- Bain A., L. Kennedy, M. Burn, A.M. Faucher. Report Archaeobotany, Palaeoclimatology and Archaeoentomology in Barbuda. Barbuda Historical Ecology Project. May 2010. (2010)

- Bain A., A.M. Faucher, L. M. Kennedy, A. R. LeBlanc, M. J. Burn , R. Boger and S. Perdikaris. Landscape Transformation During Ceramic Age and Colonial Occupations of Barbuda, West Indies, Environmental Archaeology, DOI: 10.1080/14614103.2017.1345115 (2017)

- Bernard P., and J. Lambert. Subduction and seismic hazard in the northern Lesser Antilles–Revision of the historical seismicity, Bull. Seismol. Soc. Am., 78(6), 1965–1983. (1988)

- Bertran P., Bonnissent D., Imbert D., Lozouet P., Serrand N., Stouvenot C. Paléoclimat des Petit Antilles depuis 4000 ans BP: l'enregistrement de la lagune de Grand-Case à Saint-Martin. Comptes Rendues Geoscience 336, 1501–1510. (2004)

- Bie L., A. Rietbrock, S. Hicks, R. Allen, J. Blundy, V. Clouard, J. Collier, J. Davidson, T. Garth, S. Goes, et al., Along-Arc Heterogeneity in Local Seismicity across the Lesser Antilles Subduction Zone from a Dense Ocean-Bottom Seismometer Network, Seismol. Res. Lett. 91, 237–247, doi: 10.1785/ 0220190147. (2019)

- Biguenet M., P. Sabatier, E. Chaumillon, C. Chagué, F. Arnaud, F. Jorissen, T. Coulombier, E. Geba, L. Cordrie, P. Vacher, A.L. Develle, E. Chalmin, F. Soufi, N. Feuillet. A 1600 year-long sedimentary record of tsunamis and hurricanes in the Lesser Antilles (Scrub Island, Anguilla), Sedimentary Geology, 2021, 105806, ISSN 0037-0738, https://doi.org/10.1016/j.sedgeo.2020.105806

- Biguenet M., P. Sabatier, E. Chaumillon, C. Chagué, F. Arnaud and N. Feuillet (2020), Sedimentary records of tsunamis and hurricanes in the Lesser Antilles, Abstract [NH004-05] presented at 2020 AGU Fall Meeting, 1-17 Dec.

- Buckley, M.L., Wei, Y., Jaffe, B.E., and Watt, S.G., 2012, Inverse modeling of velocities and inferred cause of overwash that emplaced inland fields of boulders at Anegada, British Virgin

Islands: Natural Hazards, v. 63, p. 133–149, doi:10.1007/s11069-011-9725-8.

- Burn MJ, Holmes J, Kennedy LM, Bain A, Marshall JD, Perdikaris S. A sediment-based reconstruction of Caribbean effective precipitation during the 'Little Ice Age' from Freshwater Pond, Barbuda. The Holocene. 2016;26(8):1237-1247. doi:10.1177/0959683616638418 (2016)

- Calais E., S. Symithe, B. Mercier de Lépinay, C. Prépetit. Plate boundary segmentation in the northeastern Caribbean from geodetic measurements and Neogene geological observations, Comptes Rendus Geoscience, Volume 348, Issue 1, 2016, Pages 42-51, ISSN 1631-0713, https://doi.org/10.1016/j.crte.2015.10.007. (2016)

- Chaytor, J.D. and ten Brink, U.S. Event sedimentation in low-latitude deep-water carbonate basins, Anegada passage, northeast Caribbean. Basin Res, 27: 310-335. https://doi.org/10.1111/bre.12076. (2015)

- Clouard, V., Roger, J., and Moizan, E.. Tsunami deposits in Martinique related to the 1755 Lisbon earthquake, Nat. Hazards Earth Syst. Sci. Discuss. https://doi.org/10.5194/nhess-2017-238, 2017.

- Cordrie, L., Gailler, A., Escalin, J. et al. Simulation of the 2004 tsunami of Les Saintes in Guadeloupe (Lesser Antilles) using new source constraints. Nat Hazards 103, 2103–2129 (2020). https://doi.org/10.1007/s11069-020-04073-x

- Cox R., Kalle L. Jahn, Oona G. Watkins, Peter Cox, Extraordinary boulder transport by storm waves (west of Ireland, winter 2013–2014), and criteria for analysing coastal boulder deposits, Earth-Science Reviews, Volume 177, 2018, Pages 623-636, ISSN 0012-8252, https://doi.org/10.1016/j.earscirev.2017.12.014.

- Cox, R., O'Boyle, L. & Cytrynbaum, J. Imbricated Coastal Boulder Deposits are Formed by Storm Waves, and Can Preserve a Long-Term Storminess Record. Sci Rep 9, 10784 (2019). https://doi.org/10.1038/s41598-019-47254-w

- Chagué-Goff C., Przemyslaw Niedzielski, Henri K.Y. Wong, Witold Szczuciński, Daisuke Sugawara, James Goff, Environmental impact assessment of the 2011 Tohoku-oki tsunami on the Sendai Plain, Sedimentary Geology, Volume 282, 2012, Pages 175-187, ISSN 0037-0738, https://doi.org/10.1016/j.sedgeo.2012.06.002.

- Craig T.J., A. Copley, J. Jackson. A reassessment of outer-rise seismicity and its implications for the mechanics of oceanic lithosphere, Geophysical Journal International, Volume 197, Issue 1, April, 2014, Pages 63–89, https://doi.org/10.1093/gji/ggu013 (2014)

- Demets C., P. Jansma, G. Mattioli, T. Dixon, F. Farina, R. Bilham, E. Calais, P. Mann. GPS geodetic constraints on Caribbean-NorthAmerica Plate Motion. Geophysical Research Letters. 27. 437- 440.10.1029/1999GL005436. (2000)

- Deplus Christine (1998) AGUADOMAR cruise, RV L'Atalante, https://doi.org/10.17600/98010120

- DEPLUS Christine, BOUDON Georges (2002) CARAVAL cruise, RV L'Atalante, https://doi.org/10.17600/2010030

- Dorel, J. Seismicity and seismic gap in the Lesser Antilles arc and earthquake hazard in Guadeloupe, Geophys. J. Roy. Astr. Soc., 67, 679–695, (1981)

- Donnelly, J.P., Webb, T. Back-barrier sedimentary records of intense hurricane landfalls in the northeastern United States (2004) Hurricanes and Typhoons: Past, Present and Future, pp. 58-95. edited by R. Murnane and K. B. Liu, Columbia Univ. Press, New York

- Donnelly, J.P. Evidence of past intense tropical cyclones from backbarrier salt pond sediments: A case study from Isla de Culebrita, Puerto Rico, USA (2005) Journal of Coastal Research, 21 (SPEC. ISS. 42), pp. 201-210.

- Donnelly, J.P., Butler, J., Roll, S., Wengren, M., Webb III, T. A backbarrier overwash record of intense storms from Brigantine, New Jersey (2004) Marine Geology, 210 (1-4), pp. 107-121. doi: 10.1016/j.margeo.2004.05.005

- Donnelly J.P. Woodruff J.D. 2007, Intense hurricane activity over the past 5,000 years controlled by El Niño and the West African monsoon: Nature , 447, p.465–468,doi: 10.1038/nature05834.

- Engel M., May S.M. Bonaire's boulder fields revisited: Evidence for Holocene tsunami impact on the Leeward Antilles. Quaternary Science Reviews 54, 126–141. (2012)

- Engel M., Brückner H., Wennrich V., Scheffers A., Kelletat D., Vött A., Schäbitz F., Daut G., Willershäuser T., May S.M. Coastal stratigraphies of eastern Bonaire (Netherlands Antilles): new insights into the palaeo-tsunami history of the southern Caribbean. Sedimentary Geology 231, 14–30. (2012)

- Engel, M., Brückner, H., Messenzehl, K. *et al.* (2012) Shoreline changes and high-energy wave impacts at the leeward coast of Bonaire (Netherlands Antilles). *Earth Planet Sp* **64,** 9 (2012). https://doi.org/10.5047/eps.2011.08.011

- Engel M., Oetjen J., May S.M., Brückner H. Tsunami deposits of the Caribbean – Towards an improved coastal hazard assessment, Earth Science Reviews, doi: 10.1016/j.earscirev.2016.10.010 (2016)

- Farías M., Comte D., Roecker S., Carrizo D., Pardo M. Crustal extensional faulting triggered by the 2010 Chilean earthquake: The Pichilemu Seismic Sequence. Tectonics 30: TC6010. (2011)

- Feuillet Nathalie (2009) GWADASEIS cruise, RV Le Suroît, https://doi.org/10.17600/9020020

- Feuillet N., Sismotectonique des Petites Antilles: Liaison entre activité sismique et volcanique, Ph.D. thesis, 283 pp., Univ. Paris VII, Paris, (2000)

- Feuillet N., I. Manighetti, P. Tapponnier, and E. Jacques. Arc parallel extension and localization of volcanic complexes in Guadeloupe, Lesser Antilles, J. Geophys. Res.,107(B12), 2331, doi:10.1029/2001JB000308, (2002)

- Feuillet N., F. Beauducel, E. Jacques, P. Tapponnier, B. Delouis, B. Delouis, S. Bazin, M. Vallée and G. C. P. King. The Mw = 6.3, November 21, 2004, Les Saintes earthquake (Guadeloupe): Tectonic setting, slip model and static stress changes,. Journal of Geophysical Research : Solid Earth, American Geophysical Union, 116 (B10), pp.B10301, doi : 10.1029/2011JB008310, (2011)(a)

- Feuillet N., F. Beauducel, and P. Tapponnier. Tectonic context of moderate to large historical earthquakes in the Lesser Antilles and mechanical coupling with volcanoes, J. Geophys. Res., doi:10.1029/2011JB008443, (2011)(b)

- Fuentes Z., Tuttle M.P., Schmidt W.E.. Sand Scripts of Past Tsunamis in Coastal Ponds of St.Thomas, https://doi.org/10.1785/0220170038. U.S. Virgin Islands. Seismological Research Letters 88, 1516– 1526. (2017)

- Fujiwara O., Akira Aoshima, Toshiaki Irizuki, Tsuke Ono, Stephen P. Obrochta, Yoshikazu Sampei, Yoshiki Sato, Ayumi Takahashi, Tsunami deposits refine great earthquake rupture extent and recurrence over the past 1300 years along the Nankai and Tokai fault segments of the Nankai Trough, Japan, Quaternary Science Reviews, Volume 227, 2020, 105999, ISSN 0277-3791, https://doi.org/10.1016/j.quascirev.2019.105999.

- Ge Z., Nemec W., Vellinga A.J. and Gawthorpe R.L. How is a turbidite actually deposited? Science Advances, eabl9124, v.8, https://doi.org/10.1126/sciadv.abl9124. (2022)

- Grindlay N.R., Mann P., and Dolan J.F. Researchers investigate submarine faults north of Puerto Rico: Eos (Transactions, American Geophysical Union), v. 78, p. 404. (1997)

- Grindlay N.R., Mann P., Dolan J.F., and van Gestel J-P. Neotectonics and subsidence of the northern Puerto Rico–Virgin Islands margin in response to the oblique subduction of high-standing ridges, in Mann, P., ed., Active tectonics and seismic hazards of Puerto Rico, the Virgin Islands, and offshore areas: Geological Society of America Special Paper 385, p. 31–60. (2005)

- Hananto N.D., F. Leclerc, L. Li, M. Etchebes, H. Carton, P. Tapponnier, Y. Qin, P. Avianto, S.C. Singh, S. Wei. Tsunami earthquakes: Vertical pop-up expulsion at the forefront of subduction megathrust, Earth and Planetary Science Letters, Volume 538, 2020, 116197, ISSN 0012-821X, https://doi.org/10.1016/j.epsl.2020.116197. (2020)

- Harada, T., S. Murotani, and K. Satake (2013), A deep outer-rise reverse-fault earthquake immediately triggered a shallow normal-fault earthquake: The 7 December 2012 off-Sanriku earthquake (MW 7.3), Geophys. Res. Lett., 40,4214–4219, doi:10.1002/grl.50808

- Hasegawa and Nakajima. Seismic imaging of slab metamorphism and genesis of intermediate-depth intraslab earthquakes. Progress in Earth and Planetary Science (2017) 4:12 DOI 10.1186/s40645-017-0126-9

- Hébert H., A. Sladen, and F. Schindelé. Numerical modeling of the great 2004 Indian Ocean tsunami: focus on the Mascarene Islands. Bulletin of the Seismological Society of America, 97(1A), (2007)

- Hébert H., D. Reymond, Y. Krien, et al., The 15th August 2007 Peru earthquake and tsunami: influence of the source characteristics on the tsunami heights. Pure and Applied Geophysics, 166, 211232, doi: 10.1007/s00024-008-0439-0, (2009)

- Heinrich P., F. Schindele, S. Guibourg and P.F. Ihmle. Modeling of the February 1996 Peruvian Tsunami. Geophysical Research Letters, 25(14), 26872690, (1998)

- Heinrich P., A. Jamelot, A. Cauquis, A. Gailler, Taitoko, an advanced code for tsunami propagation, developed at the French Tsunami Warning Centers, European Journal of Mechanics - B/Fluids, Volume 88, 2021, Pages 72-88, ISSN 0997-7546, https://doi.org/10.1016/j.euromechflu.2021.03.001.

- Huang S.Y., Yen J.Y., Wu B.L. and Shih N.W. (2020). Field observations of sediment transport across the rocky coast of east Taiwan: Impacts of extreme waves on the coastal morphology by Typhoon Soudelor. Marine Geology, Volume 421, 2020, 106088, ISSN 0025-

3227, https://doi.org/10.1016/j.margeo.2019.106088.

- Hurukawa N., B.R. Wulandari, M. Kasahara. Earthquake History of the Sumatran Fault, Indonesia, since 1892, Derived from Relocation of Large Earthquakes. Bulletin of the Seismological Society of America ; 104 (4): 1750–1762. doi: https://doi.org/10.1785/0120130201 (2014)

- Jessen C.A., Pedersen J.B.T., Bartholdy J., Seidenkrantz M.S. and Kuijpers A. A late Holocene palaeoenvironmental record from Altona Bay, St. Croix, US Virgin Islands, Geografisk Tidsskrift-Danish Journal of Geography, 108:2, 59-70, DOI: 10.1080/00167223.2008.10649589 (2008)

- Jolivet R., Simons, M., Duputel, Z., Olive, J.-A., Bhat, H. S., & Bletery, Q. (2020). Interseismic loading of subduction megathrust drives long-term uplift in Northern Chile. Geophysical Research Letters, 47, e2019GL085377. https://doi.org/10.1029/2019GL085377

- Kennedy A. B., Nobuhito Mori, Yao Zhang, Tomohiro Yasuda, Shen-En Chen, Yoshimitsu Tajima, William Pecor & Kinya Toride (2016). Observations and Modeling of Coastal Boulder Transport and Loading During Super Typhoon Haiyan, Coastal Engineering Journal, 58:1, 1640004-1-1640004-25, DOI: 10.1142/S0578563416400040

- Krien, Y., Dudon, B., Roger, J., Arnaud, G., and Zahibo, N.: Assessing storm surge hazard and impact of sea level rise in the Lesser Antilles case study of Martinique, Nat. Hazards Earth Syst. Sci., 17, 1559–1571, https://doi.org/10.5194/nhess-17-1559-2017, 2017.

- Kumar A., Lara S. Wagner, Susan L. Beck, Maureen D. Long, George Zandt, Bissett Young, Hernando Tavera, Estella Minaya, Seismicity and state of stress in the central and southern Peruvian flat slab, Earth and Planetary Science Letters, Volume 441, 2016, Pages 71-80, ISSN 0012-821X, https://doi.org/10.1016/j.epsl.2016.02.023.

- LAIGLE Mireille, LEBRUN Jean Frédéric, HIRN Alfred (2007) SISMANTILLES 2 cruise, RV L'Atalante, https://doi.org/10.17600/7010020

- Lander J.F., L.S. Whiteside, and P.A. Lockridge. A brief history of tsunami in the Caribbean Sea. Science of Tsunami Hazards, v. 20, 57-94, (2002)

- Lane Chad S., Jeffrey J. Clark, Andrew Knudsen, Jamie McFarlin, Late-Holocene paleoenvironmental history of bioluminescent Laguna Grande, Puerto Rico, Palaeogeography, Palaeoclimatology, Palaeoecology, Volume 369, 2013, Pages 99-113, ISSN 0031-0182, https://doi.org/10.1016/j.palaeo.2012.10.007.

- Laurencin M., B. Marcaillou, D. Graindorge, F. Klingelhoefer, S. Lallemand, M. Laigle, and J.-F. Lebrun. The polyphased tectonic evolution of the Anegada Passage in the northern Lesser Antilles subduction zone, Tectonics, 36, 945–961, doi:10.1002/2017TC004511 (2017)

- Laurencin M., D. Graindorge, F. Klingelhoefer, B. Marcaillou, M. Evain. Influence of increasing convergence obliquity and shallow slab geometry onto tectonic deformation and seismogenic behavior along the Northern Lesser Antilles zone, Earth and Planetary Science Letters, Volume 492, 2018, Pages 59-72, ISSN 0012-821X, https://doi.org/10.1016/j.epsl.2018.03.048. (2018)

- Lavigne, F., Paris, R., Grancher, D. et al. Reconstruction of Tsunami Inland Propagation on December 26, 2004 in Banda Aceh, Indonesia, through Field Investigations. Pure appl. geophys. 166, 259–281 (2009). https://doi.org/10.1007/s00024-008-0431-8

- Lay, T., Ammon, C., Kanamori, H. et al. The 2009 Samoa–Tonga great earthquake triggered doublet. Nature 466, 964–968 (2010). https://doi.org/10.1038/nature09214

- Leclerc F., N. Feuillet, and C. Deplus. Interactions between active faulting, volcanism, and sedimentary processes at an island arc: Insights from Les Saintes channel, Lesser Antilles arc: Geochemistry, Geophysics, Geosystems, v. 17, no. 7, p.27812802, doi:10.1002/2016GC006337, (2016)

- Leclerc F. et Feuillet N. Quaternary coral reef complexes as markers of long-term subduction-induced subsidence. Geosphere, Geological Society of America, 2019,

doi:10.1130/GES02069.1. hal-02361011, (2019)

- Le Friant, A., Heinrich, P., and Boudon, G. (2008), Field survey and numerical simulation of the 21 November 2004 tsunami at Les Saintes (Lesser Antilles), Geophys. Res. Lett., 35, L12308, doi:10.1029/2008GL034051.

- MacInnes, B., Kravchunovskaya, E., Pinegina, T., & Bourgeois, J. (2016). Paleotsunamis from the central Kuril Islands segment of the Japan-Kuril-Kamchatka subduction zone. Quaternary Research, 86(1), 54-66. doi:10.1016/j.yqres.2016.03.005

- Malaizé B., Bertran P., Carbonel P., Bonnissent D., Charlier K., Galop D., Imbert D., Serrand N., Stouvenot C., Pujol C. Hurricanes and climate in the Caribbean during the past 3700 years BP. The Holocene 21, 911–924 (2011)

- Manaker D.M., Calais E., Freed A.M., Ali S.T., Przybylski P., Mattioli G., Jansma P., Prépetit C., de Chabalier, J.B.. Interseismic Plate coupling and strain partitioning in the northeastern Caribbean. Geophys. J. Int. 174 (3), 889–903. (2008)

- Marcaillou, B., Klingelhoefer, F., Laurencin, M. *et al.* Pervasive detachment faults within the slow spreading oceanic crust at the poorly coupled Antilles subduction zone. *Commun Earth Environ* **2,** 203 (2021). https://doi.org/10.1038/s43247-021-00269-6

- McCann W.R. and Sykes L.R. Subduction of aseismic ridges beneath the Caribbean Plate: implications for the tectonics and seismic potential of the northeastern Caribbean. J. Geophys. Res. 89 (B6), 4493– 4519. (1984)

- Morena P., Antonio Cattaneo, Gueorgui Ratzov, Frauke Klingelhoefer, Arthur Bieber, et al.. Deep megadeposits as paleoseismic indicators in the Lesser Antilles subduction zone. EGU General Assembly, Apr 2019, Vienne, Austria. pp.2019 - 15192, ⟨10.17600/16001800⟩. ⟨hal-02383782⟩

- Morton R.A., Richmond B.M., Jaffe B.E., Gelfenbaum G. Reconnaissance investigation of Caribbean extreme wave deposits – preliminary observations, interpretations, and research

directions. USGS Open-File Report 2006-1293. (2006)

- Morton, R.A., Richmond, B.M., Jaffe, B.E., and Gelfenbaum, G., 2008, Coarse-clast ridge complexes of the Caribbean: A preliminary basis for distinguishing tsunami and storm-wave origins: Journal of Sedimentary Research, v. 78, p. 624–637, doi:10.2110/jsr.2008.068.

- Morton R. A., Guy Gelfenbaum, Mark L. Buckley, Bruce M. Richmond, Geological effects and implications of the 2010 tsunami along the central coast of Chile, Sedimentary Geology, Volume 242, Issues 1–4, 2011, ages 34-51, ISSN 0037-0738, https://doi.org/10.1016/j.sedgeo.2011.09.004.

- Mouslopoulou, V., O. Oncken, S. Hainzl, and A. Nicol (2016), Uplift rate transients at subduction margins due to earthquake clustering, Tectonics, 35, 2370–2384, doi:10.1002/2016TC004248.

- Nikitina Daria L., Andrew C. Kemp, Benjamin P. Horton, Christopher H. Vane, Orson van de Plassche, Simon E. Engelhart, Storm erosion during the past 2000years along the north shore of Delaware Bay, USA, Geomorphology, Volume 208, 2014, Pages 160-172, ISSN 0169-555X, https://doi.org/10.1016/j.geomorph.2013.11.022.

- Okada Y. Surface deformation due to shear and tensile faults in a half-space. Bulletin of the Seismological Society of America, 75(4):1135, (1985)

- Palmer S.E., Burn M.J. and Holmes J. A multiproxy analysis of extreme wave deposits in a tropical coastal lagoon in Jamaica, West Indies. Nat Hazards 104, 2531–2560. https://doi.org/10.1007/s11069- 020-04284-2 (2020)

- Paris R., Jérôme Fournier, Emmanuel Poizot, Samuel Etienne, Julie Morin, Franck Lavigne, Patrick Wassmer, Boulder and fine sediment transport and deposition by the 2004 tsunami in Lhok Nga (western Banda Aceh, Sumatra, Indonesia): A coupled offshore–onshore model, Marine Geology, Volume 268, Issues 1–4, 2010, Pages 43-54, ISSN 0025-3227, https://doi.org/10.1016/j.margeo.2009.10.011.

- Paris R., Patrick Wassmer, Junun Sartohadi, Franck Lavigne, Benjamin Barthomeuf, Emilie Desgages, Delphine Grancher, Philippe Baumert, Franck Vautier, Daniel Brunstein, Christopher Gomez C., Tsunamis as geomorphic crises: Lessons from the December 26, 2004 tsunami in Lhok Nga, West Banda Aceh (Sumatra, Indonesia), Geomorphology, Volume 104, Issues 1–2, 2009, Pages 59-72, ISSN 0169-555X, https://doi.org/10.1016/j.geomorph.2008.05.040.

- Paris R., P. Sabatier, M. Biguenet, A. Bougouin, G. André, J. Roger (2021). A tsunami deposit at Anse Meunier, Martinique Island: Evidence of the 1755 CE Lisbon tsunami and implication for hazard assessment, Marine Geology, Volume 439, 2021, 106561, ISSN 0025-3227, https://doi.org/10.1016/j.margeo.2021.106561.

- Paulatto, M. et al., Dehydration of subducting slow-spread oceanic lithosphere in the Lesser Antilles. Nat. Commun. 8, 15980 doi: 10.1038/ncomms15980 (2017)

- Philibosian B., N. Feuillet, J. Weil-Accardo, E. Jacques, A. Guihou, A.S. Mériaux, A. Anglade, J.M. Saurel, S. Deroussi. 20th-century strain accumulation on the Lesser Antilles megathrust based on coral microatolls. Earth and Planetary Science Letters, Volume 579, 117343, ISSN 0012-821X, (2022)

- Pignatelli C., Scheffers A., Scheffers S., Mastronuzzi G. Assessment of extreme wave flooding from geomorphologic evidence in Bonaire (Netherlands Antilles). Zeitschrift für Geomorphologie 54 (Suppl. 3), 219–245. (2010)

- Poupardin A., P. Heinrich, H. Hébert, F. Schindelé, A. Jamelot, D. Reymond, H. Sugioka. Traveltime delay relative to the maximum energy of the wave train for dispersive tsunamis propagating across the Pacific Ocean: the case of 2010 and 2015 Chilean Tsunamis. Geophysical Journal International., 214. 10.1093/gji/ggy200, (2018)

- Radtke U., Schellmann G., Scheffers A., Kelletat D., Kromer B., Kasper H.U. Electron spin resonance and radiocarbon dating of coral deposited by Holocene tsunami events on Curaçao, Bonaire and Aruba (Netherlands Antilles). Quaternary Science Reviews 22, 1309–

1315. (2003)

- Reid H.F. and Taber S. The Virgin Islands earthquakes of 18671868, Bull. Seismol. Soc. Am., 10, 930, (1920)

- Reymond D., E. Okal, H. Hébert and M. Bourdet. Rapid forecast of tsunami wave heights from a database of pre-computed simulations, and application during the 2011 Tohoku tsunami in French Polynesia, Geophys. Res. Lett., 39, L11603, doi:10.1029/2012GL051640, (2012)

- Robson G.R. An earthquake catalogue for the eastern Caribbean 1530-1960. Bulletin of the Seismological Society of America. Vol. 54, No. 2, pp. 785-832. April, 1964

- Rogers G.C. and H.S. Hasegawa. A second look at the British Columbia earthquake of June 23, 1946. Bulletin of the Seismological Society of America, Vol. 68, No. 3, pp. 653-675, June, 1978. (1978)

- Roger J., S. Allgeyer, H. Hebert, M. A. Baptista, A. Loevenbruck, F. Schindele. The 1755 Lisbon Tsunami in Guadeloupe Archipelago: Source Sensitivity and Investigation of Resonance Effects. The Open Oceanography Journal, 2010, 4: 58-70. DOI: 10.2174/1874252101004010058

- Roger, J., Baptista, M.A., Sahal, A. et al. The Transoceanic 1755 Lisbon Tsunami in Martinique. Pure Appl. Geophys. 168, 1015–1031 (2011). https://doi.org/10.1007/s00024-010-0216-8

- Ruiz S., R. Madariaga, Historical and recent large megathrust earthquakes in Chile, Tectonophysics, Volume 733, 2018, Pages 37-56, ISSN 0040-1951, https://doi.org/10.1016/j.tecto.2018.01.015.

- Rusydy I., Idris Y., Mulkal et al., Shallow crustal earthquake models, damage, and loss predictions in Banda Aceh, Indonesia. Geoenviron Disasters 7, 8. https://doi.org/10.1186/s40677-020-0145-5. (2020)

- Sainte-Claire Deville M.Ch. Observations sur le tremblement de terre éprouvée la Guadeloupe le 8 février 1843, (1843)

- Sainte-Claire Deville M.Ch. Sur le tremblement de terre du 18 novembre 1867 aux Antilles. Comptes Rendus, Acad. Sci., Paris, v. 65, 1110-1114, (1867)

- Santibáñez I., Cembrano J., García-Pérez T., Costa C., Yáñez G., Marquardt C., Arancibia G., González G. Crustal faults in the Chilean Andes: geological constraints and seismic potential., Andean Geology 46 (1): 32-65. doi:http://dx.doi.org/10.5027/andgeoV46n1-3067 (2018)

- Sawai, Y., Y. Namegaya, Y. Okamura, K. Satake, and M. Shishikura (2012), Challenges of anticipating the 2011 Tohoku earthquake and tsunami using coastal geology, Geophys. Res. Lett., 39, L21309, doi:10.1029/2012GL053692

- Seibert C., N. Feuillet, G. Ratzov, C. Beck, A. Cattaneo, Seafloor morphology and sediment transfer in the mixed carbonate-siliciclastic environment of the Lesser Antilles forearc along Barbuda to St. Lucia, Marine Geology, Volume 428, 2020, 106242, ISSN 0025-3227, https://doi.org/10.1016/j.margeo.2020.106242.

- Seibert, C., Feuillet, N.; Beck, C.; Ducassou, E.; Morena, P.; Johannes, L.; Ratzov, G.; Goldfinger, C.; Cattaneo, A.; Moreno, E. “Long Term Recurrence of Deeply Ponded Turbidites and Thick Homogenites in the Lesser Antilles Forearc: Imprint of Great Earthquakes”, 2019. AGU Fall Meeting Abstracts

- Scheffers A. Paleotsunami in the Caribbean: field evidences and datings from Aruba, Curaçao and Bonaire. Essener Geographische Arbeiten 33. (2002)

- Scheffers A. Kelletat D. Sedimentologic and geomorphologic tsunami imprints worldwide a review. Earth-Science Reviews 63, 83–92. (2003)

- Scheffers A. Tsunami imprints on the Leeward Netherlands Antilles (Aruba, Curaçao, Bonaire) and their relation to other coastal problems. Quaternary International 120, 163–172.

(2004)

- Scheffers A., Scheffers S., Kelletat D. Paleo-tsunami relics on the southern and central Antillean Island Arc. Journal of Coastal Research 21, 263–273. (2005)

- Scheffers A. Kelletat D. New evidence and datings of Holocene paleo-tsunami events in the Caribbean (Barbados, St. Martin and Anguilla), in: Mercado-Irizarry, A., Liu, P. (Eds.), Caribbean tsunami hazard. World Scientific, Singapore, pp. 178–202. (2006)

- Schindelé F., A. Gailler, H. Hébert et al., Implementation and Challenges of the Tsunami Warning System in the Western Mediterranean. Pure Appl. Geophys. 172, 821833, doi:10.1007/s00024-014- 0950-4, (2015)

- Shepherd J.B. Tsunami hazard in the Eastern Caribbean. Workshop on Volcanic and Seismic Hazards in the Eastern Caribbean (May 28 June 1, 2001), (2001).

- Shepherd J.B. and L.L. Lynch. An earthquake catalogue for the Caribbean, Part I., The pre-instrumental period, 1502-1990. Paper presented to the Steering Committee, Latin American and Caribbean Seismic Hazard Programme, April, 60 pp. (1992)

- Spiske M., Böröcz Z., Bahlburg H. The role of porosity in discriminating between tsunami and hurricane emplacement of boulders – A case study from the Lesser Antilles, southern Caribbean. Earth and Planetary Science Letters 268, 384–396. (2008)

- Spiske, M. (2016) Coral-rubble ridges as dynamic coastal features — short-term reworking and weathering processes: Advances in Geosciences, v. 38, doi:10.5194/adgeo-38-55-2016.

- Spiske, M., Garcia Garcia, A.-M., Tsukamoto, S. and Schmidt, V. (2020), High-energy inundation events versus long-term coastal processes – room for misinterpretation. Sedimentology, 67: 1460-1480. https://doi.org/10.1111/sed.12524

- Spiske M., Tang H., Bahlburg H. (2020). Post-depositional alteration of onshore tsunami deposits – Implications for the reconstruction of past events, Earth-Science Reviews, Volume 202, 2020, 103068, ISSN 0012-8252, https://doi.org/10.1016/j.earscirev.2019.103068.

- Spiske, M., Pilarczyk, J.E., Mitchell, S., Halley, R.B. & Otai, T. (2021) Coastal erosion and sediment reworking caused by hurricane Irma – implications for storm impact on low-lying tropical islands. *Earth Surface Processes and Landforms*, 1– 17. Available from: https://doi.org/10.1002/esp.5293

- Stein S., J. F. Engeln, and D. A. Wiens. Subduction seismicity and tectonics in the lesser Antilles arc, J. Geophys. Res., 87, 86428664, (1982)

- Styron, R., García-Pelaez, J., and Pagani, M.: CCAF-DB: the Caribbean and Central American active fault database, Nat. Hazards Earth Syst. Sci., 20, 831–857, https://doi.org/10.5194/nhess-20-831-2020, 2020.

- Symithe S., Calais E., de Chabalier J.-B., Robertson R., Higgins M. Current block motions and strain accumulation on active faults in the Caribbean. J. Geophys. Res. 120, 1–27. (2015)

- ten Brink U., W. Danforth, C. Polloni, B. Andrews, P. Llanes, S. Smith, E. Parker, and T. Uozumi. New seafloor map of the Puerto Rico trench helps assess earthquake and tsunami hazards, Eos Trans. AGU, 85, 349–360, doi:10.1029/2004EO370001. (2004)

- ten Brink U. Vertical motions of the Puerto Rico Trench and Puerto Rico and their cause, J. Geophys. Res., 110, B06404, doi:10.1029/2004JB003459. (2005)

- Ulrich T., Gabriel AA., Ampuero JP. et al., Dynamic viability of the 2016 Mw 7.8 Kaikōura earthquake cascade on weak crustal faults. Nat Commun 10, 1213. https://doi.org/10.1038/s41467-019-09125-w (2019)

- van Hengstum, P. J., Donnelly, J. P., Fall, P. L., Toomey, M. R., Albury, N. A., & Kakuk, B. (2016). The intertropical convergence zone modulates intense hurricane strikes on the western North Atlantic margin. Scientific Reports, 6(October 2015), 21728. https://doi.org/10.1038/srep21728

- van Rijsingen E., Calais E., Jolivet R., de Chabalier J. B., Jara J., Symithe S., et al., Inferring

Interseismic Coupling along the Lesser Antilles Arc: a Bayesian Approach. Journal of Geophysical Research: Solid Earth, 125, e2020JB020677https://doi.org/10.1029/2020JB020677. (2020)

- Wallace, E. J., Donnelly, J. P., van Hengstum, P. J., Winkler, T. S., McKeon, K., MacDonald, D., et al. (2021). 1,050 years of hurricane strikes on Long Island in The Bahamas. Paleoceanography and Paleoclimatology, 36, e2020PA004156. https://doi.org/10.1029/2020PA004156

- Wang K., and Y. Hu. Accretionary prisms in subduction earthquake cycles: The theory of dynamic Coulomb wedge, J. Geophys. Res., 111, B06410, doi:10.1029/2005JB004094. (2006)

- Watt S.G., Jaffe B.E., Morton R.A., Richmond B.M., Gelfenbaum G. Description of extreme-wave deposits on the northern coast of Bonaire, Netherlands Antilles. USGS Open-File Report 2010-1180. (2010)

- Weil-Accardo, J., Feuillet, N., Jacques, E., Deschamps, P., Beauducel, F., Cabioch, G., Tapponnier, P., Saurel, J.-M., and Goleńzka, J. Two hundred thirty years of relative sea level changes due to climate and megathrust tectonics recorded in coral microatolls of Martinique (French West Indies), J. Geophys. Res. Solid Earth, 121, 2873– 2903, doi:10.1002/2015JB012406. (2016).

- Wells D.L. and K.J. Coppersmith. New empirical relationships among magnitude, rupture length, rupture width, rupture area, and surface displacement. Bulletin of the Seismological Society of America, 84(4):974, (1994)

- Wells E.C., S.M. Pratt, G.L. Fox, P.E. Siegel, N.P. Dunning and A.R. Murphy. Plantation Soilscapes: Initial and Cumulative Impacts of Colonial Agriculture in Antigua, West Indies, Environmental Archaeology, DOI: 10.1080/14614103.2017.1309806. (2017)

- Witter, R. C., G. A. Carver, R. W. Briggs, G. Gelfenbaum, R. D. Koehler, S. P. La Selle, A.

M. Bender, S. E. Engelhart, E. Hemphill-Haley, and T. D. Hill. Unusually large tsunamis frequent a currently creeping part of the Aleutian megathrust, Geophys. Res. Lett., 43, 76–84, doi:10.1002/2015GL066083, (2016).

- Witter R. C., Rich Briggs, Simon E. Engelhart, Guy Gelfenbaum, Rich D. Koehler, Alan Nelson, SeanPaul La Selle, Reide Corbett, Kristi Wallace; Evidence for frequent, large tsunamis spanning locked and creeping parts of the Aleutian megathrust. GSA Bulletin 2019;; 131 (5-6): 707–729. doi: https://doi.org/10.1130/B32031.1

- Woodruff Jonathan D., Jeffrey P. Donnelly, David Mohrig, Wayne R. Geyer; Reconstructing relative flooding intensities responsible for hurricane-induced deposits from Laguna Playa Grande, Vieques, Puerto Rico. Geology 2008;; 36 (5): 391–394. doi: https://doi.org/10.1130/G24731A.1

- Yue H., Lay T., Rivera L., Bai Y., Yamazaki Y., Cheung K.F., Hill E.M., Sieh K., Kongko W., Muhari A. Rupture process of the 2010 M w 7.8 Mentawai tsunami earthquake from joint inversion of near-field hr-GPS and teleseismic body wave recordings constrained by tsunami observations. J. Geophys. Res., Solid Earth 119 (7), 5574–5593 (2014)

- Zahibo N., E. Pelinovsky, E. Okal, A. Yalçiner, C. Kharif, T. Talipova and A. Kozelkov. The earthquake and tsunami of November 21, 2004 at Les Saintes, Guadeloupe, Lesser Antilles, Science of Tsunami Hazards, Vol. 23, No. 1, 25-39, (2005)

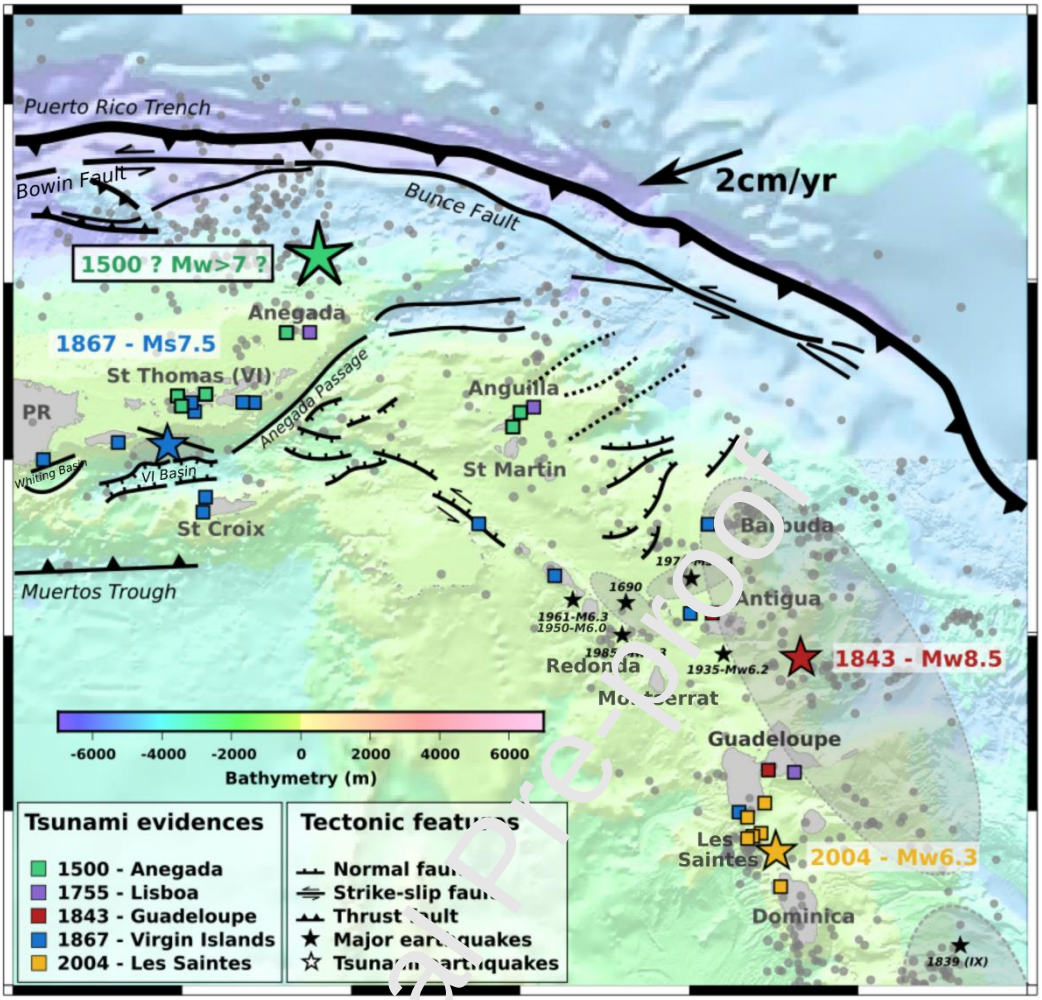

Figure 1 : Location of tsunami evidences in the Lesser Antilles*. Black stars indicate major past earthquakes. Colored squares the position of tsunami evidence.*

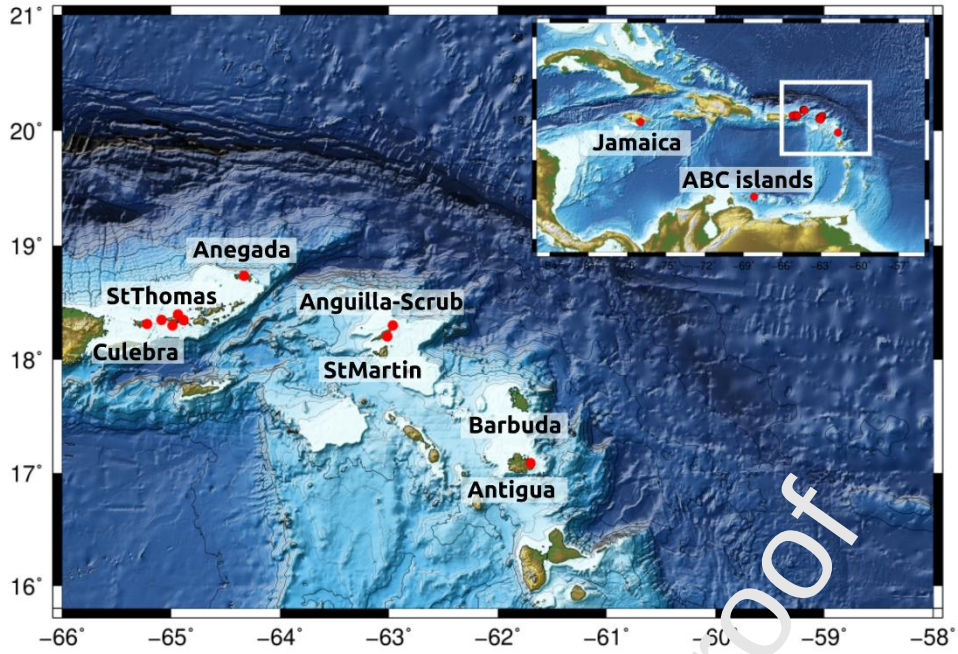

Figure 2 : *Map of tsunami deposits dating from a time range around 1450 CE. Red circles indicate the position of the boulders, sand deposits and event in cores. ABC islands correspond to Aruba, Bonaire and Curaçao, most of the deposits are identified on Bonaire island.*

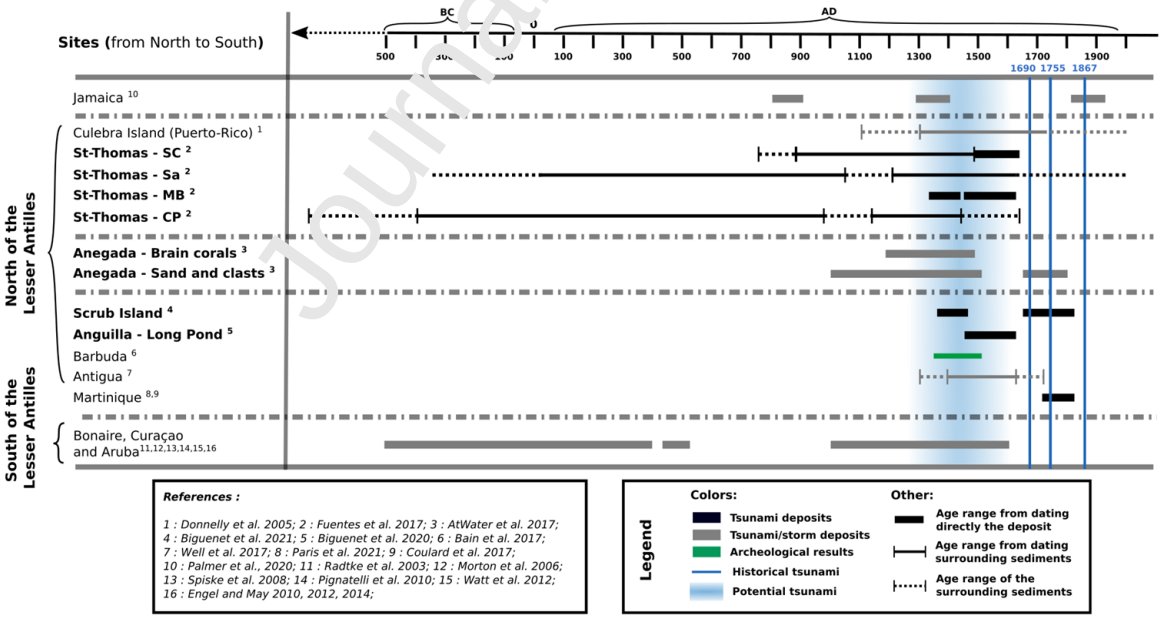

Figure 3 *: Graphic of the age and locations of tsunami and/or hurricane deposits identified in the Caribbean Sea area. The deposits are listed with details in Table 1.*

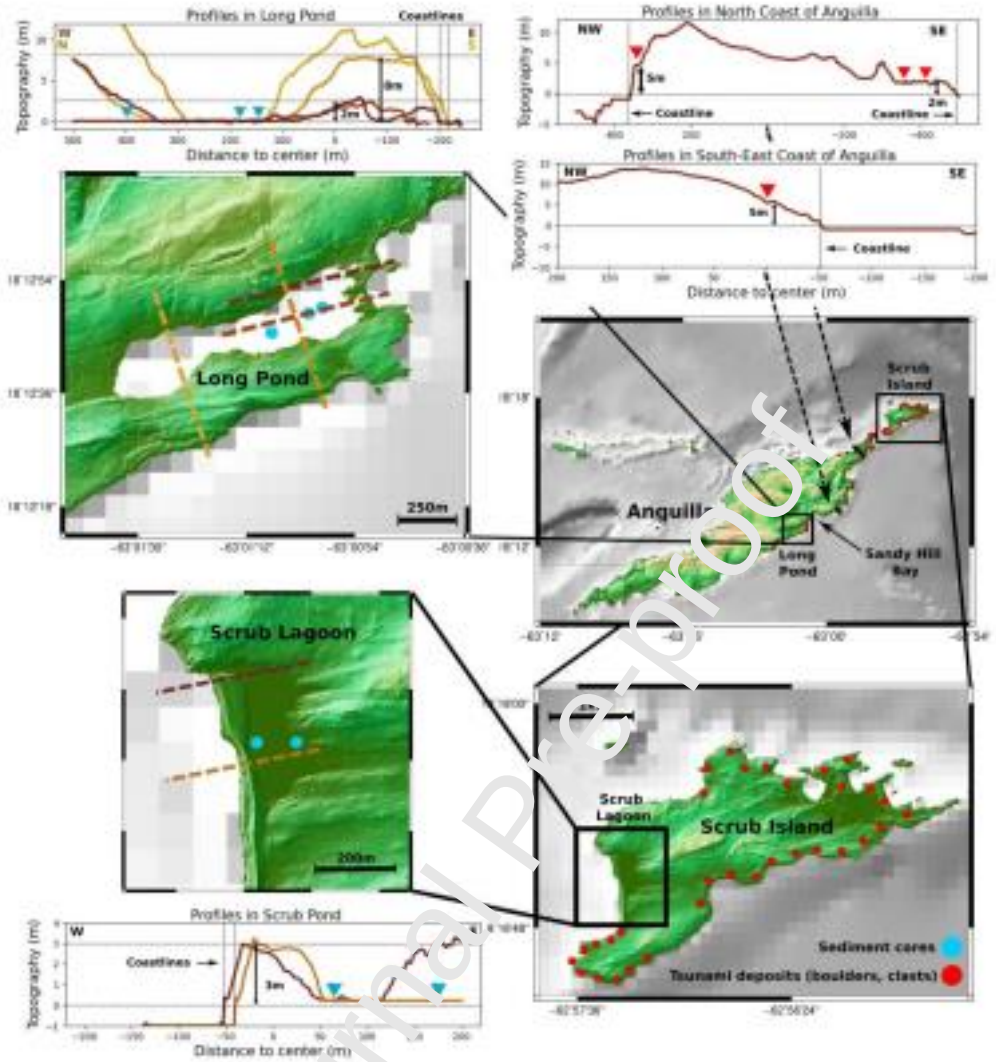

Figure 4 : *Maps of Anguilla and Scrub Islands with topographic profiles*

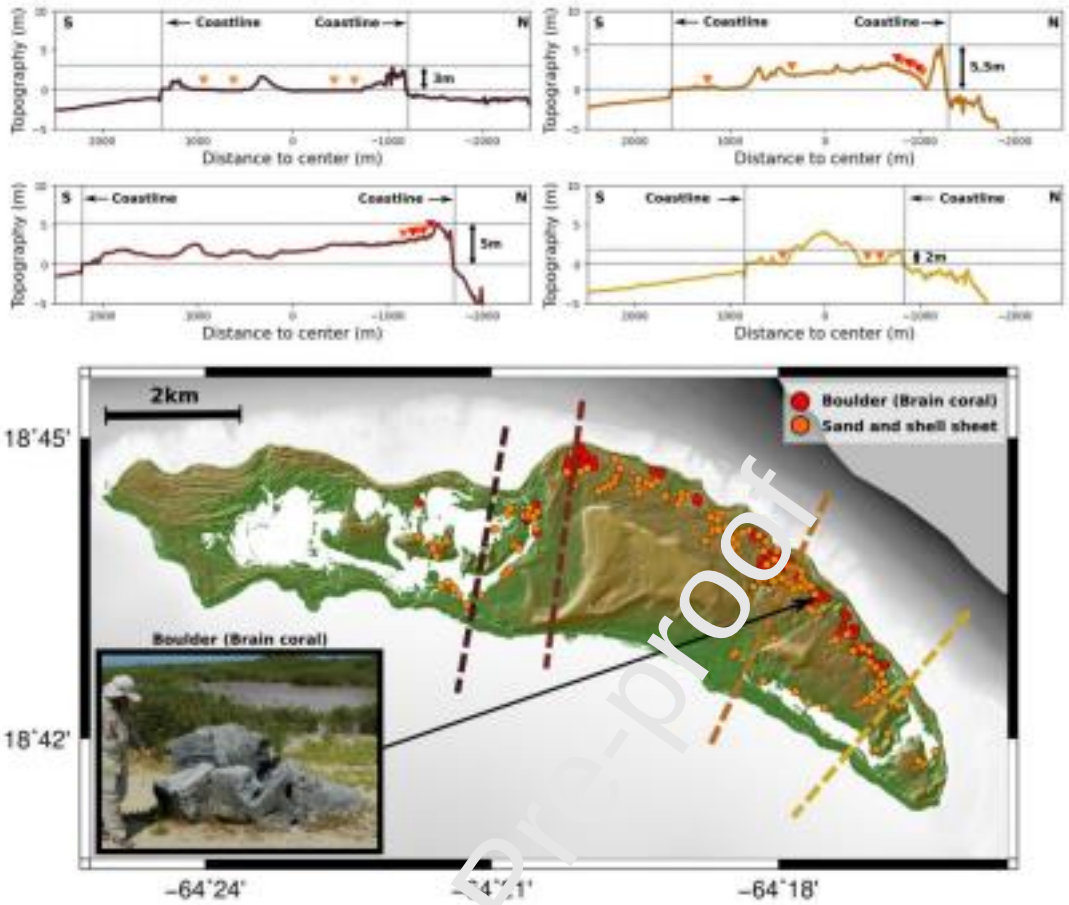

Figure 5 *: Map of Anedaga Island with topographic profiles and deposits locations. and deposits locations.*

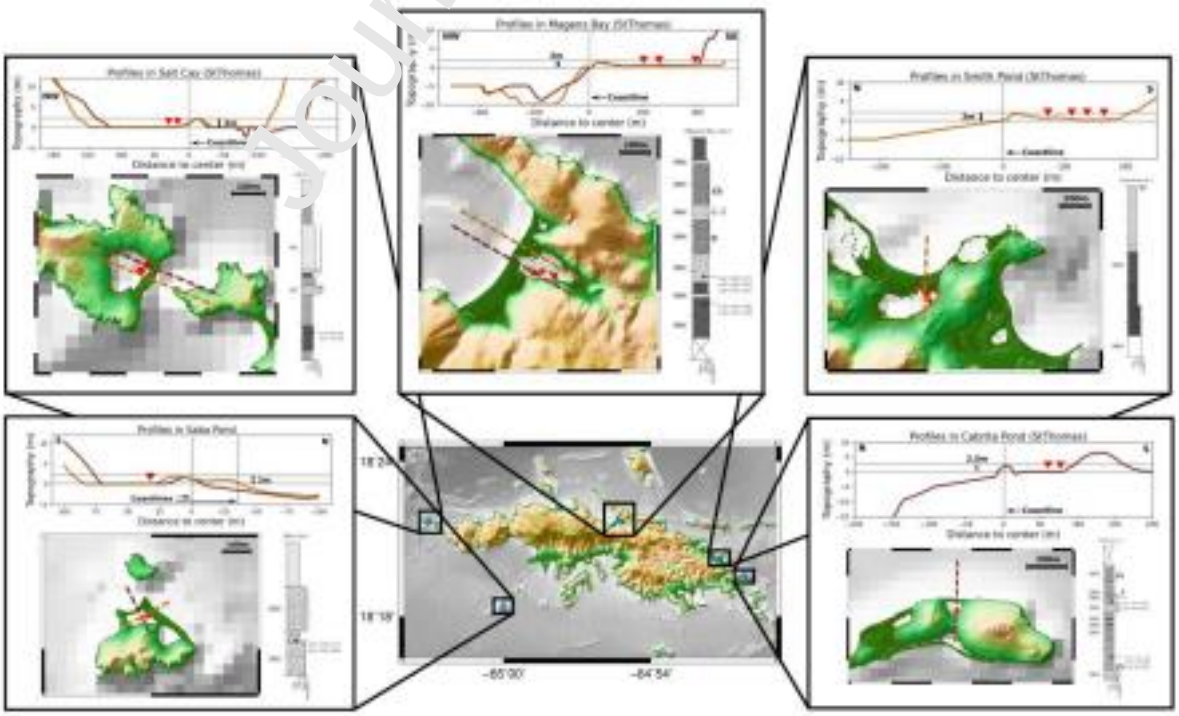

Figure 6 : *Maps of Saint-Thomas Island with topographic profiles at deposits locations*

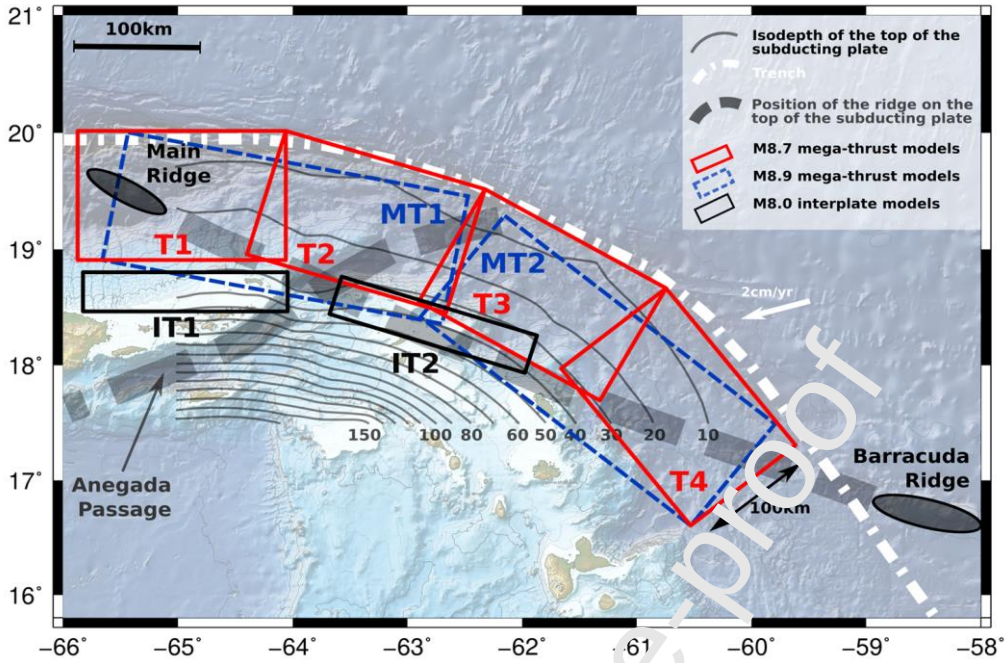

Figure 7 : Map of the subduction fault models. *The rectangle represents the surface projection of the faults, the 200 km long in red ('T' for thrust), the 350 km long in blue ('MT' for mega-thrust) and the deep interplate in black ('IT') (see parameters in Table 2). The black dotted ribbon between Barracuda Ridge and Main Ridge is the extension of these ridges under the Caribbean plate, on the top of the subducting slab. The second black dotted ribbon corresponds to the Anegada Passage, the limit between Puerto-Rico micro plate and the Caribbean plate.*

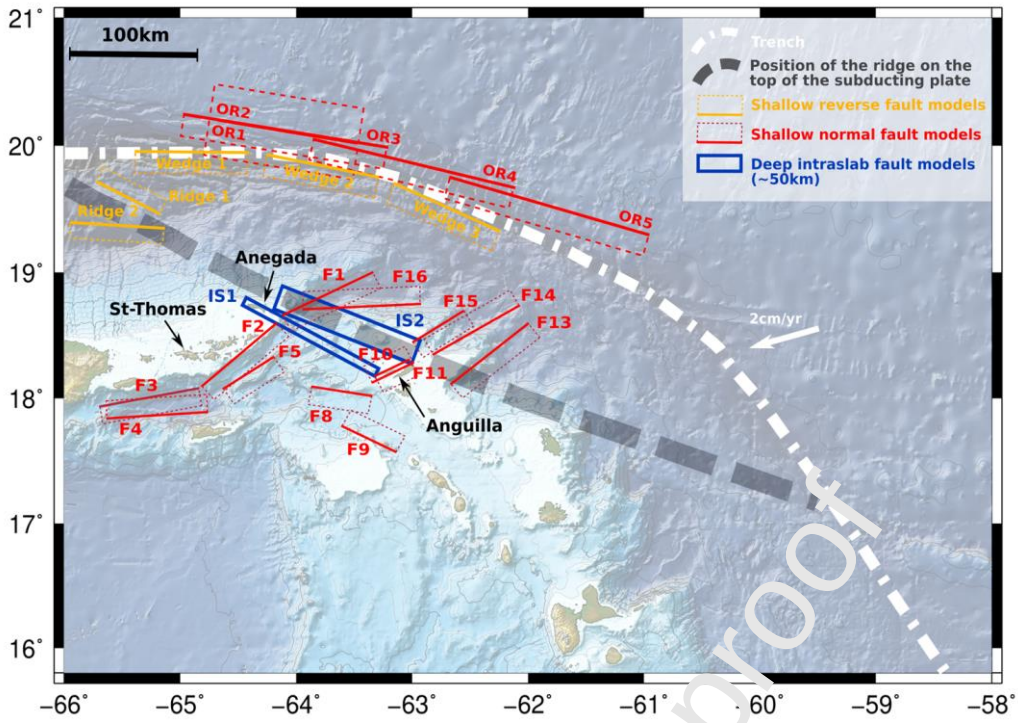

Figure 8 : Map of the crustal fault, wedge fault and intraslab fault models. *The plain lines represent the surface rupture and the dotted rectangle the surface projection of the fault. The 'F' faults are the intra-arc fault models, the 'Ridge' and 'OuterRise' are the crustal trench models, the 'Wedge' are the wedge fault models and 'IS' are the deep intraslab fault models (see parameters in Table 2).*

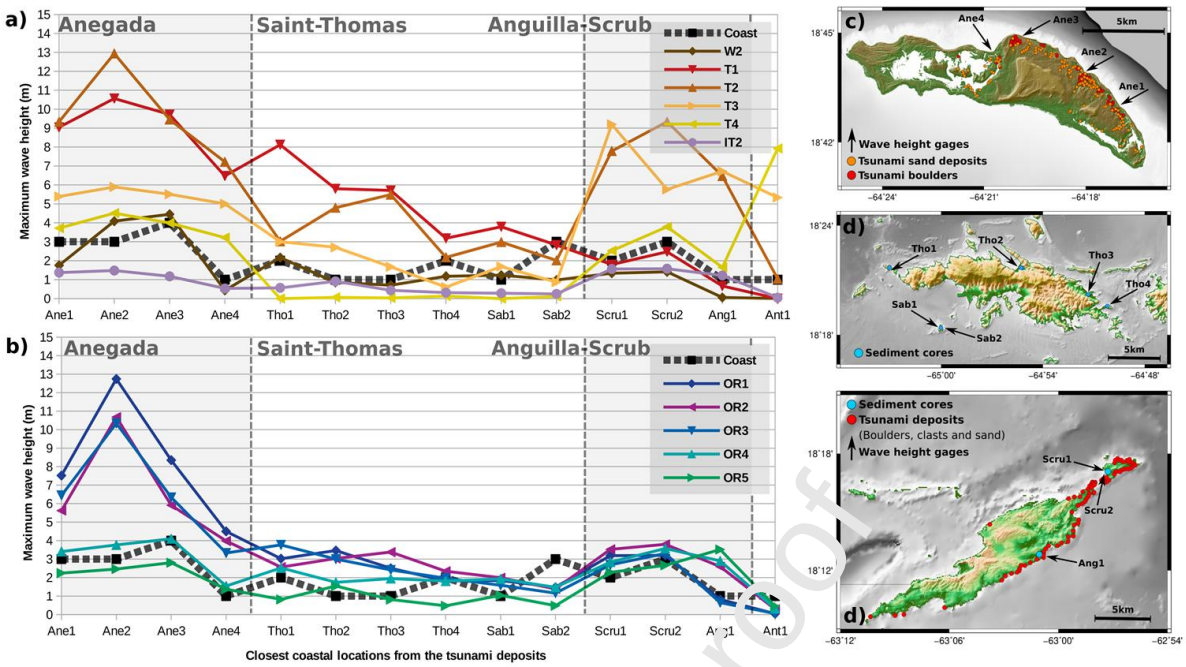

Figure 9 : Maximal water heights on the coastline generated by some of the fault models*. The curves are divided in two graphics for more readability: the thrust and intraplate models in (a) and the crustal models in (b). The positions are the closest point (offshore) to the most important deposit locations of the three areas (Anegada, Saint-Thomas and Anguilla). Each position is indicated by the arrows on the three maps (c, d, e). The black dotted curve in a) and b) graphics correspond to the topography of the coast at the location.*

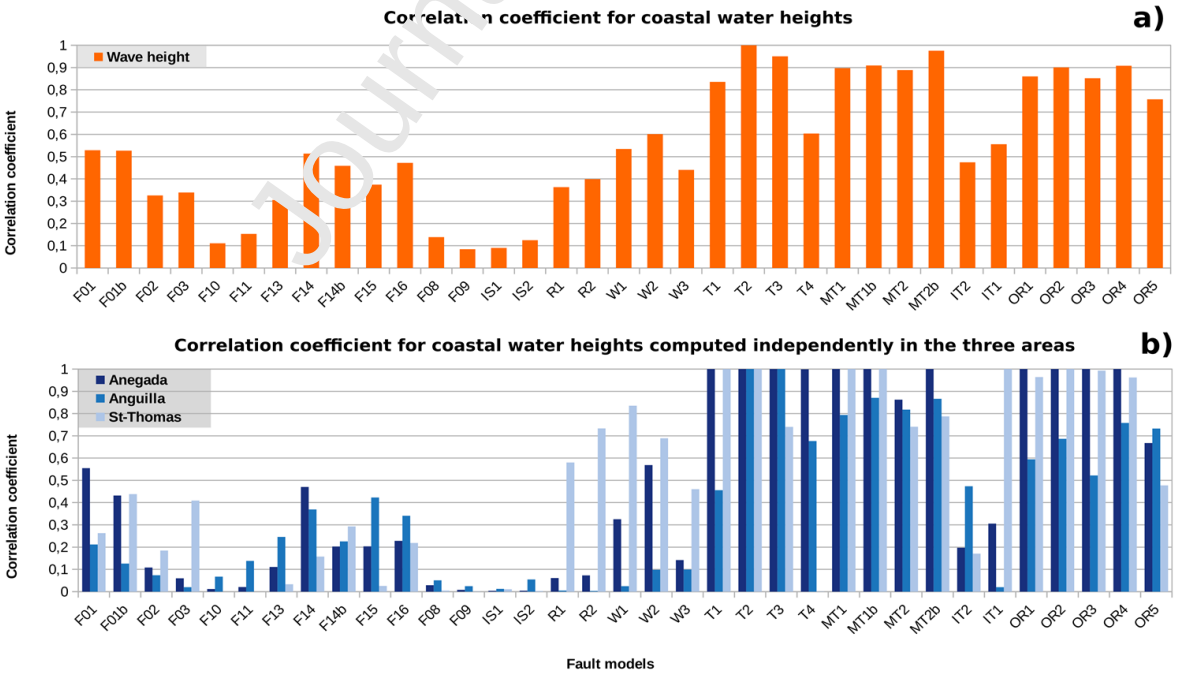

Figure 10 : Histograms of the correlation coefficient computed for each fault model between the

***simulated water heights and the tsunami deposits locations**. a) Correlation coefficients computed for the wave heights at the coastline before run-up. b) Correlation coefficients computed for the wave heights at the coastline before run-up on Anegada (dark blue), on Anguilla and Scrub (middle blue) and Saint Thomas (light blue). Fault models parameters are listed in Table 2 : Parameters of the fault models (Okada models).*

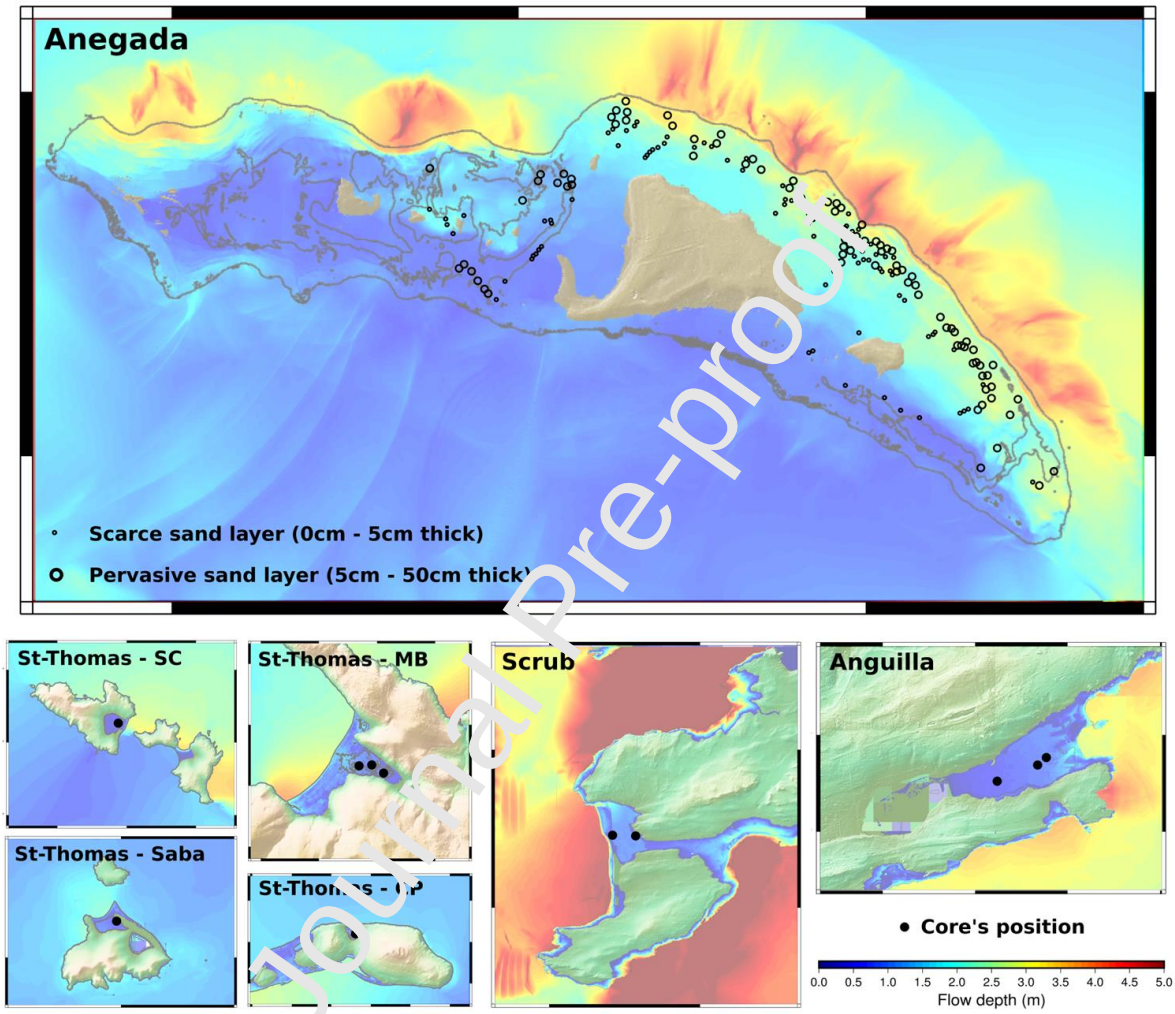

***Figure 11 : Model T2 flow depth maps at the deposition sites of Anegada, Anguilla, Scrub and Saint-Thomas.** The flow depth values on-land correspond to the maximal water thickness above the ground and the values offshore correspond to maximal water height above sea level (0). The green and brown areas correspond to the topography of the unflooded part of the islands.*

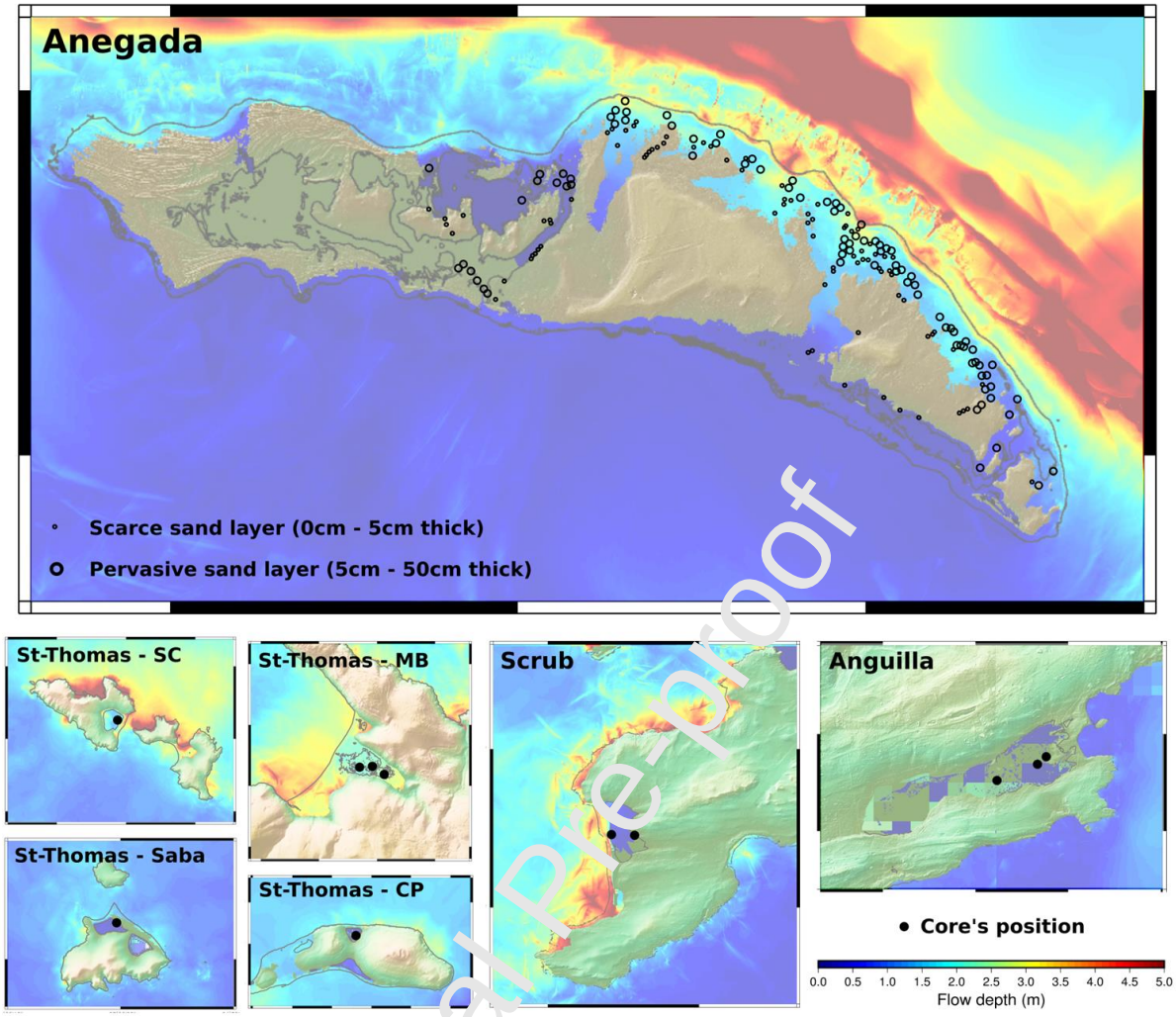

Figure 12 : Model OR3 flow depth maps at the deposition sites of Anegada, Anguilla, Scrub and Saint-Thomas. *The flow depth values on-land correspond to the maximal water thickness above the ground and the values offshore correspond to maximal water height above sea level (0). The green and brown areas correspond to the topography of the unflooded part of the islands.*

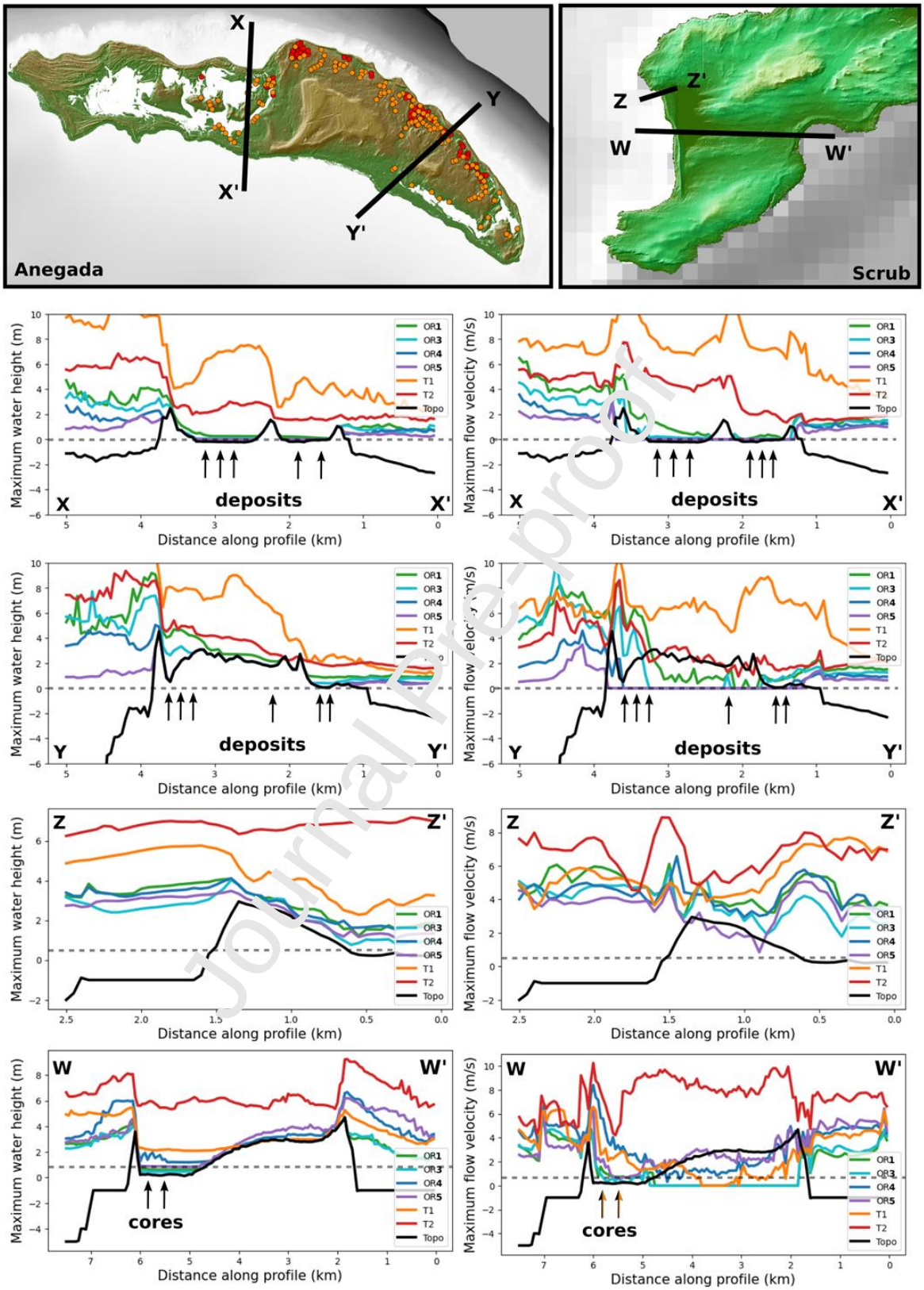

Figure 13 : *Top maps: bathymetric and topographic maps of Anegada and Scrub with the sections used for the profiles indicated in black. Graphics: maximum water height (left) and velocity (right) profiles obtained for models OR1, OR3, OR4, OR5, T1 and T2. The values are extracted from the four sections XX', YY', ZZ' and*

WW', the black curve corresponds to the topographic profile, the dashed line indicates the zero sea level and the arrows indicate the position of the 1200-1500 cal yrs CE tsunami deposits..

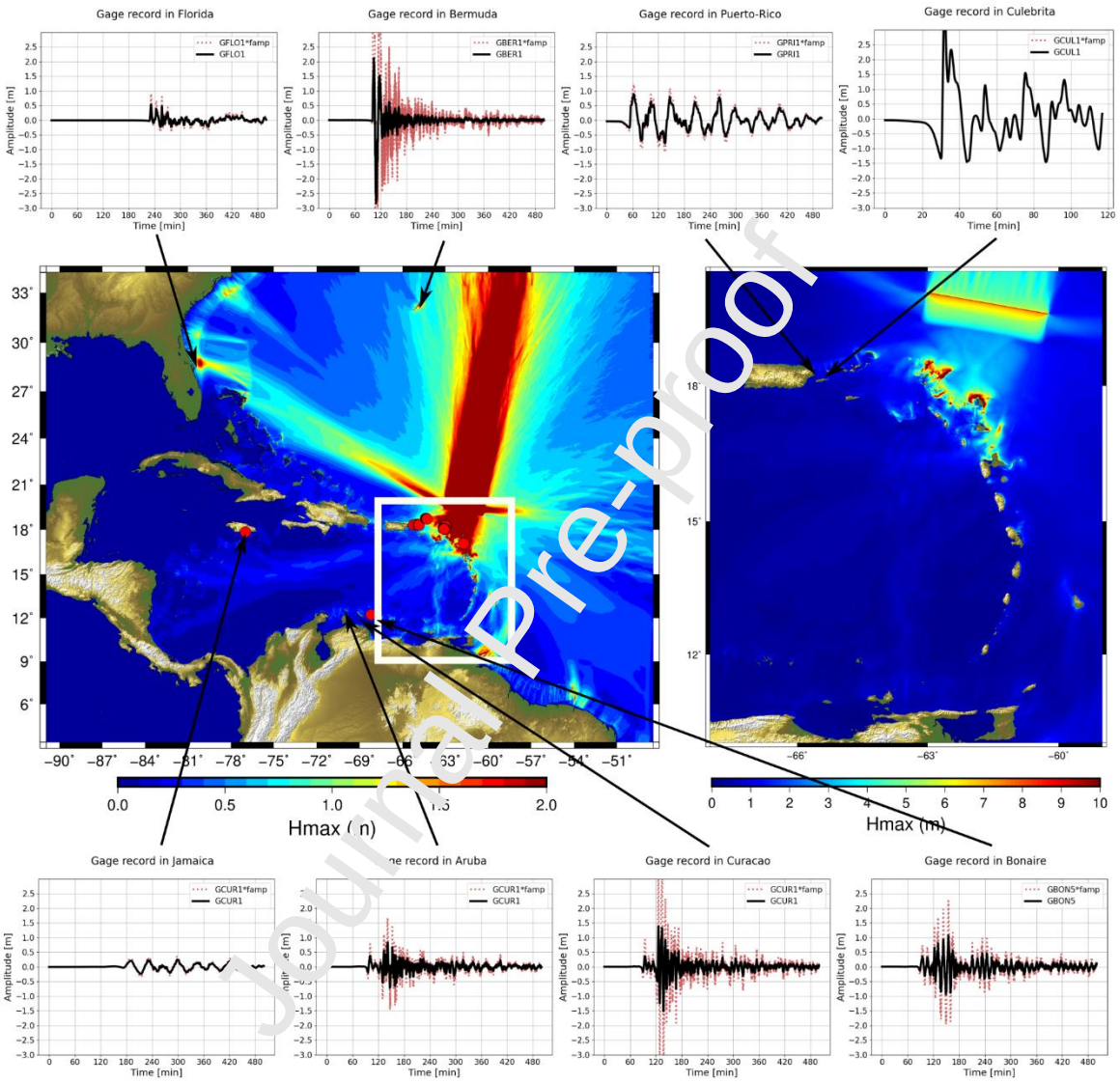

Figure 14 : Maximal water height map and synthetic waveforms from the far-field simulation of model MT1. *The simulation was performed on a 500 m resolution grid from GEBCO (2020) data base. The left map corresponds to maximal water height modeled on the Caribbean Sea and surroundings with a water height scale saturated at 2 m. The right map is the zoom on the Antilles Arc with a water height scale saturated at 10 m. The graphics correspond to the waveforms computed at the coasts of Florida, Jamaica, Bonaire Island, Barbados and Bermuda. The red points are the tsunami deposits dating from a period around 1450AD.*

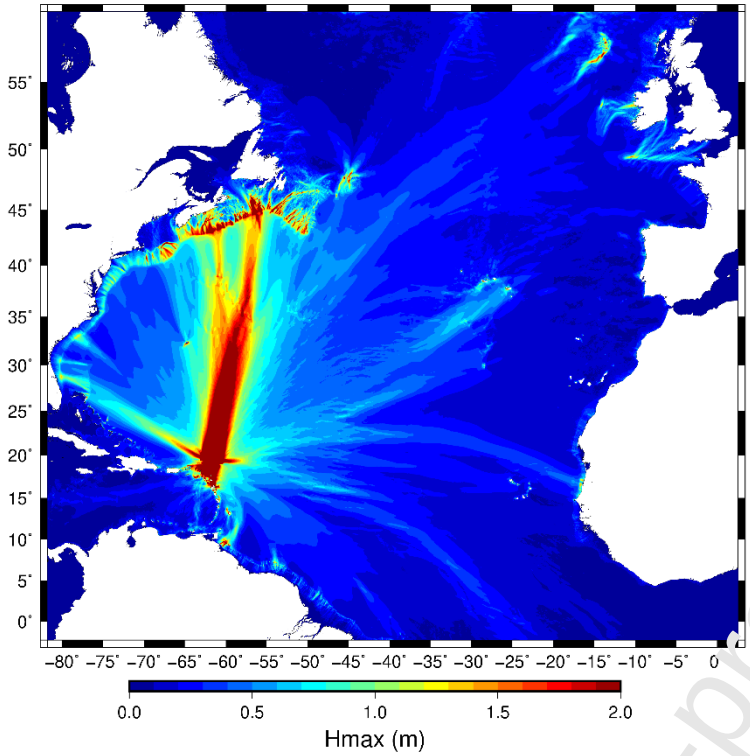

Figure 15 : Maximal water height map of the Atlantic coasts from the simulation of model MT1*. White areas correspond to continental areas.*

Table 1 : List and characteristics of the overwash deposits. The deposits are listed from the North to the South of the Lesser Antilles. The position coordinates (Lat, Lon) are in degrees. The age ranges are plotted in Figure 3 and those indicated in bold are the Pre-Columbian one used in this study. TD means Tsunami Deposit. The tsunami evidences are citations from the associated referenced articles. The heights are extracted from the bathymetric grids as indicated in Figures 4, 5 and 6.

Places	Position	Traces	Dates (CE)	Tsunami or storm (criteria)	Height	References
Jamaica	**17.850190, -76.986663**	13 cores from a lagoon with four overwash layers: one storm, one tsunami and two uncertain deposits	1691–1730 or 1810–1934	**Tsunami** : « It comprises marine bioclasts and Ostracods...that are mixed with lagoonal microfossils...» « sedimentary evidence of rafted marine organic fragments... and associated peaks in iron counts »	Beach ridge of 1 to 4m high	Palmer et al. 2020
			Between 1290 and 1400	**Likely storm but not excluding tsunami**		
			Older than 768–900	**Likely storm but not excluding tsunami**		
Culebrita (Puerto-Rico)	**18.320312, -65.236235 18.320411, -65.236488 18.320233, -65.236500**	3 cores from a pond : several overwash layers including known hurricane deposits but other deposits associated to more intense events	**Younger than 1700**	**Storm or tsunami** : « Thick layer of sandy shell (20cm) with abrupt contacts » « Given the previous work on differences between tsunami and storm-induced deposits, no sedimentary structures in the Big Culebrita Salt Pond archive point to tsunami deposition. Nevertheless tsunami-induced deposition cannot be ruled out. »		Donelly et al. 2005
Saint-Thomas Salt Cay	**18.361589, -65.050579 18.361413, -65.050748**	2 cores with three overwash layers: one storm and two tsunami deposits (TD)	TD1 ~ 1484 - 1645 (leaf)	**Tsunami:** "The layers showed mixed composition (marine and lacustrine), erosional contacts, fining upward sequences, and the presence of a mud cap at some sites and were interpreted as tsunami deposits"	Beach ridges of 2 to 3m high	Fuentes et al. 2017
			760-882 > TD2 > 1484-1645 (younger than wood dated at 760-882 and older than leaf at 1484-1645)			
Saint-Thomas Saba Pond	**18.306540, -65.000208**	1 core with two overwash layers: two tsunami deposits (TD)	**1042-1221 > TD1 > ?** (younger than wood dated at 1221–1042)		Beach ridges of 1 to 3m high	
			? > TD2 > 1042-1221 (older than a wood dated at 1221–1042)			
Saint-Thomas Magen Bay	**18.361072, -64.920255 18.361340, -64.921047 18.361306, -64.921618**	3 cores with two overwash layers: two tsunami deposits (TD)	TD1 ~ 1441-1630 (leaf)		Beach ridges of 1 to 2m high	
			TD2 ~ 1329-1445 (wood)			
Saint-Thomas Smith Pond	**18.336935, -64.855233 18.336800, -64.855372 18.336897, -64.855420 18.337019, -64.855463**	4 cores with two overwash layers: two tsunami deposits (TD)	TD1 : no dates		Beach ridges of 1 to 2m high	
			TD2: no dates			

Saint-Thomas Cabrita Pond	**18.326256, -64.836742 18.326383, -64.836656**	2 cores with nine overwash layers: seven storm and two tsunami deposits (TD)	**983-1151 > TD1 > 1445-1631 (younder than twig dated at 983-1151 and older than a wood dated at 1445-1651)** 737-401 BC > TD2 > 983-1151 CE (younger than wood dated at 737-401 BC and older than twig dated at 983-1151 CE)		Beach ridges of 1 to 2m high	
Anegada	**18.737615, -64.393281 to 18.691936, -64.273443**	Sand sheet and shells	Sand sheet and shells dated from 1650-1800	**Tsunami or storm** : « The sand and shell sheet might represent tsunami overwash, hurricane overwash waves generated inside the marine pond, and the opening of tidal channels. Reinhardt et al. (2012) found that among these possibilities, tsunami overwash best explains this sheet's lateral extent and form. » Interpreted as the 1755 Lisbon tsunami	Deposits at 0 to 6m asl	AtWater et al. 2017
		Huge amount of deposits : 200 boulders, clasts, sand layers...	**Sand sheet and shells with 56 clasts dated from 1000-1200** **10 brain corals dated from 1200-1480 with diameters of 0.5 m to 2.7 m (among more than 200 coral boulders identified mostly on the northern coast)**	**Tsunami or storm** : « A tsunami probably emplaced both of the fields of scattered limestone boulders and cobbles… Emplacement by storm was deemed unlikely on the basis of location far inland and elongation perpendicular to shore. A category 5 hurricane was found insufficient to produce the flows inferred by modeling transport of the largest of the boulders… before 2013 Typhoon Haiyan made clear that an unusually large storm can produce tsunami like bores in a setting like that of Anegada's north shore. »		
Anguilla	**multiple deposits**	Boulders all along the coastline	No dates	storm or tsunami	Deposits at 0 to 10m asl	Sheffers et al. 2006
	18.213421, -63.016891 18.213261, -63.017380 18.212580, -63.018681	3 cores from a lagoon : several overwash events with a tsunami deposit	**1471 – 1643 CE**	**Tsunami**	Beach ridge of 2m to 3m high	Biguenet et al. 2020
Scrubb	**multiple deposits**	Boulders all along the coastline	No dates	storm or tsunami	Deposits at 0 to 5m asl	Sheffers et al. 2006
	18.284370, -62.955341 18.284031, -62.954250	2 cores from a lagoon : 25 overwash events with two tsunami deposits	**1364 - 1469 CE**	**Tsunami** : « … sedimentological (rip-up clast of the underlying cohesive substrate and internal mud laminae), and geochemical evidence. »	Beach ridge of 2m to 5m high	Biguenet et al. 2021

Antigua	**17.070304, -61.713299**	Coarse sand and microshell deposit in a core (storm or tsuna-mi)	1350 – 1650 CE	**Storm or tsunami** : « unique coarse sand with micro-shells layer that contrast with the rest of the core »	Beach ridge of 1 to 5m high	Well et al. 2017
Barbuda		No traces	Potential island abandonnement between 1300AD and 1500AD			Burn et al. 2016 ; Bain et al. 2017

Table 2 : Parameters of the fault models (Okada models). *L refers to the fault length, W to the fault width and D to the depth of the fault center. Each letter in the models refers to a fault group: 'F' for the intra-arc faults; 'R' for the Puerto-Rico Main ridge faults; 'OR' for the Outer-Rise faults; 'W' for the wedge faults; 'T' for the interplate thrust faults; 'MT' for the interplate mega-thrust faults; 'IT' for the deep interplate faults; 'IS' for the intraslab faults.*

Fault	Length (km)	Width (km)	Depth (km)	Slip (m)	Dip (°)	Rake (°)	Mw
F01	80	20	7.1	2	45	-90	7.3
F01b	80	20	7.1	5	45	-90	7.56
F02	80	20	7.1	2	45	-90	7.3
F03	80	20	7.1	2	45	-90	7.3
F04	80	20	7.1	2	45	-90	7.3
F05	60	20	7.1	2	45	-90	7.2
F08	50	20	7.1	2	45	-90	7.15
F09	50	20	7.1	2	45	-90	7.15
F10	30	20	7.1	2	45	-90	7.02
F11	35	20	7.1	2	45	-90	7.06
F13	80	20	7.1	2	45	-90	7.3
F14	80	20	7.1	2	45	-90	7.3
F14b	80	20	7.1	5	45	-90	7.56
F15	60	20	7.1	2	45	-90	7.2
F16	100	20	7.1	2	45	-90	7.36
R1	40	20	8.7	5	60	90	7.36
R2	50	20	8.7	5	60	90	7.43
OR1	120	45	20	7	60	-90	8.0
OR2	120	45	20	7	60	-90	8.0
OR3	150	25	11	10	60	-90	8.0
OR4	150	25	11	10	60	-90	8.0
OR5	150	25	11	10	60	-90	8.0
W1	100	20	1.75	20	10	90	8.0
W2	100	20	1.75	20	10	90	8.0
W3	100	20	1.75	20	10	90	8.0
T1	200	100	9	20	10	90	8.7
T2	200	100	9	20	10	90	8.7
T3	200	100	9	20	10	90	8.7
T4	200	100	9	20	10	90	8.7

MT1	300	100	9	20	10	90	8.8
MT1b	300	100	9	30	10	90	8.9
MT2	300	100	9	20	10	90	8.8
MT2b	300	100	9	30	10	90	8.9
IT1	150	60	40	6	20	90	8.0
IT2	150	60	40	6	20	90	8.0
IS1	100	20	50	5	85	-90	7.63
IS2	100	20	50	5	35	-90	7.63

Declaration of interests

☒ The authors declare that they have no known competing financial interests or personal relationships that could have appeared to influence the work reported in this paper.

☐The authors declare the following financial interests/personal relationships which may be considered as potential competing interests: